Mechanisms producing different precipitation patterns over north-eastern Italy: insights from HyMeX-SOP1 and previous events

Article

Accepted Version

QUARTERLY JOURNAL OF THE ROYAL METEOROLOGICAL SOCIETY
RMetS Royal Meteorological Society

Mechanisms producing different precipitation patterns over North-Eastern Italy: insights from HyMeX-SOP1 and previous events

Journal:	*QJRMS*
Manuscript ID	QJ-15-0126.R2
Wiley - Manuscript type:	HyMeX Special Issue
Date Submitted by the Author:	n/a
Complete List of Authors:	Davolio, Silvio; Institue of Atmospheric Sciences and Climate (ISAC), National Research Council of Italy (CNR) Volontè, Ambrogio; University of Reading, Department of Meteorology Manzato, Agostino; ARPA FVG - OSMER, Pucillo, Arturo; ARPA FVG - OSMER, Cicogna, Andrea; ARPA FVG - OSMER, Ferrario, Massimo; ARPA Veneto,
Keywords:	heavy precipitation, orography, convection, HyMeX, Alps

Mechanisms producing different precipitation patterns over North-Eastern Italy: insights from HyMeX-SOP1 and previous events

S. Davolio[a,*], A. Volonté[b], A. Manzato[c], A. Pucillo[c], A. Cicogna[c], M. E. Ferrario[d]

[a]Institute of Atmospheric Sciences and Climate (ISAC), National Research Council of Italy (CNR), Bologna, Italy

[b]Department of Meteorology, University of Reading, UK – formerly Dep. of Physics, University of Milan, Italy

[c]ARPA Friuli Venezia Giulia – OSMER, Visco (Udine), Italy

[d]ARPA Veneto, Servizio Meteorologico, Teolo (Padua), Italy

[*]Correspondence to: S. Davolio, Institute of Atmospheric Sciences and Climate (ISAC), National Research Council of Italy (CNR), Via Gobetti 101, Bologna 40129, Italy.

E-mail: S.Davolio@isac.cnr.it

Key words: heavy precipitation, orography, HyMeX, Alps, convection

ABSTRACT

During the first HyMeX Special Observation Period (SOP1) field campaign, the target site of North Eastern Italy (NEI) experienced a large amount of precipitation, locally exceeding the climatological values and distributed among several heavy rainfall episodes. In particular, two events that occurred during the last period of the campaign drew our attention. These events had common large-scale patterns and a similar mesoscale setting, characterised by southerly low-level flow interacting with the Alpine orography, but the precipitation distribution was very different. During IOP18 (31 October – 1 November 2012), convective systems were responsible for intense rainfall mainly located over a flat area of the eastern Po Valley, well upstream of the orography. Conversely, during IOP19 (4 – 5 November 2012), heavy precipitation affected only the Alpine area. In addition to IOP18 and IOP19, the present study analyses other heavy-precipitation episodes that display similar characteristics and which occurred over NEI during the autumn of recent years. A high-resolution (2-km grid spacing) non-hydrostatic NWP model and available observations are used for this purpose.

The two different observed precipitation patterns are explained in terms of interaction between the impinging flow and the Alps. Depending on the thermodynamic profile, convection can be triggered when the impinging flow is forced to rise over a pre-existing cold-air layer at the base of the orography. In this situation persisting blocked-flow condition and upstream convergence are responsible for heavy rain localized over the plain. Conversely, if convection does not develop, flow-over conditions establish and heavy rain affects the Alps. Numerical parameters proposed in the literature are used to support the analysis.

Finally, the role of evaporative cooling beneath the convective systems is evaluated. It turns out that the stationarity of the systems upstream of the Alps is mainly attributable to persisting blocked-flow conditions, while convective outflow slightly modifies the location of precipitation.

1. Introduction

During autumn 2012, the first field campaign (Special Observation Period - SOP1, Ducrocq et al., 2014) of the international project HyMeX (Hydrological Cycle in the Mediterranean Experiment; Drobinski et al., 2014) took place with the aim of studying heavy precipitation and floods in the Mediterranean basin. The North Eastern Italy hydro-meteorological site (NEI – Figure 1) was selected from the various target areas over the Italian territory monitored during the campaign, in order to specifically investigate Alpine intense rainfall. NEI has the maximum annual-average precipitation over Italy (Frei and Schär, 1998; Isotta et al., 2013) and was also a target site in previous field campaigns (e.g. Mesoscale Alpine Programme, MAP, Bougeault et al. 2001) and projects (e.g. MAP Demonstration Phase - DPHASE, Rotach et al., 2009). Thus, SOP1 represented a sort of continuation of previous experiments, focusing mainly on the finer scales of atmospheric convection.

During autumn, the deepening of Atlantic troughs over the Mediterranean basin and the relatively high sea surface temperature combine to create atmospheric conditions conducive to heavy rainfall (Doswell et al. 1998; Massacand et al., 1998; Buzzi and Foschini, 2000; Borga et al., 2007; Manzato et al., 2015). The steep and complex orography of the Alpine area makes floods a common hazard during autumn. Autumn 2012 was no exception in this regard: several intense precipitation episodes affected NEI, which turned out to be the rainiest area of the campaign (Davolio et al., 2015). More than 1000 mm of rainfall was recorded over the Alps of the Friuli Venezia Giulia (FVG) region (see Figure 1 for the location) during the two-month period of SOP1, locally exceeding climatological values for this time of year. Two contrasting, heavy-precipitation events, thoroughly monitored during Intense Observing Periods (IOPs) 18 and 19, particularly drew our attention and prompted this study.

These two IOPs were very close in time and characterised by similar synoptic conditions and intense low-level south-easterly flow over the Adriatic Sea (typically referred to as Sirocco wind) impinging on the Alps. However, they produced quite different precipitation patterns. In IOP18 (31

October – 1 November) the development of convective systems was responsible for intense rainfall confined over a flat area of the eastern Po Valley, far upstream of the orography and close to the Adriatic coast. In contrast, during IOP 19 (4 – 5 November) heavy precipitation affected the mountainous Alpine area and only very light rainfall was recorded over the plain.

Different precipitation patterns associated with similar large-scale circulation were already identified and discussed for the north-western Alps in several studies, fostered by MAP. In particular, the characteristics of two episodes of the MAP field campaign (MAP-IOP2b and MAP-IOP8) were analysed from different perspectives (Rotunno and Ferretti, 2003; Bousquet and Smull, 2003; Rotunno and Houze, 2007). It turned out that the different thermodynamic profile of the impinging flow, and thus its different stability, allowed - or prevented - the low-level air from rising over the Alpine barrier. The different orographic flow regime - flow over or flow around (Smith, 1979) - determined the location, intensity and characteristics of the precipitation. During MAP-IOP2b heavy orographic rainfall with embedded convection affected the Alpine slopes, while during MAP-IOP8 weak stratiform and long-lasting precipitation was widespread over the Po Valley.

More recently, Barbi et al. (2012) provided a detailed description of four convective episodes affecting the coastal area of the Veneto region (part of NEI, Figure 1) far from the Alpine orography. These events occurred in September of four consecutive years and the associated large rainfall totals represented a peculiar feature in the climatology of the region, which is characterised by maximum annual values over the Alps and lower annual values, but with high occurrence of heavy rainfall, over the plain. In accordance with the finding of Monai et al. (2006) and Davolio et al. (2009b), the authors highlighted the importance of the orographic flow modification: the south-easterly low-level flow from the Adriatic Sea was blocked and deflected ahead of the Alps, resulting in a north-easterly barrier wind over the plain (Schwerdtfeger, 1984; Di Muzio, 2014). This barrier wind converged with the impinging south-easterly flow near the coastal area and this

low-level convergence, together with conditionally instability, was responsible for initiating and sustaining organised convection.

Conversely, in the NEI Pre-Alpine and Alpine area, higher values of annual accumulated precipitation are closely linked to direct orographic uplift of the southerly moisture-laden airflow from the Adriatic Sea, responsible for long-lasting orographic precipitation. Recent flooding episodes over NEI, also mentioned briefly in Barbi et al. (2012), fit within this category of events, which includes typical autumnal heavy rainfall affecting the southern side of the Alps.

In the present study, attention is focussed on the period between September and November, when the climatological peak of heavy precipitation is in the north-western Mediterranean (Ducrocq et al., 2014), and specifically over NEI (Manzato, 2015). This peak is caused by the higher frequency of Atlantic storms entering the Mediterranean and aided by additional heat and moisture provided by the relatively warm Adriatic Sea. Over NEI, during this period there is a progressive transition from summer convective weather, associated with conditionally unstable flow, to the so-called flux precipitation (Manzato, 2007) typical of long-lasting, sometimes flood-producing, events along the southern side of the Alps and associated with near-neutral moist stratification (Miglietta and Rotunno, 2005; Malguzzi et al., 2006).

In addition to IOP18 and IOP19 of the HyMeX-SOP1 mentioned above, other heavy-precipitation episodes displaying similar precipitation patterns and affecting NEI are selected and analysed in this study. The aim is to investigate and better understand possible common thermodynamic mechanisms that modulate the precipitation pattern for the two categories of analysed events and to define analytical parameters able to describe the physical processes associated with the two observed orographic flow regimes.

The paper is organised as follows. After a description of the employed numerical models and of the simulation strategy (Section 2), the results of a detailed investigation of the events, based on both observations and high-resolution model simulations, are summarised in Section 3. Section 4

presents the main findings concerning physical mechanisms playing a key role in different phases of the events. Finally, conclusions are drawn in Section 5.

2. Model description

The Numerical Weather Prediction (NWP) system employed in the present study is based on the hydrostatic BOlogna Limited Area Model (BOLAM) and the non-hydrostatic MOdello LOCale in Hybrid coordinates (MOLOCH), developed by the Institute of Atmospheric Sciences and Climate of the Italian National Research Council (CNR – ISAC). The two models are being used operationally at ISAC as part of an agreement with the National Civil Protection Department and also at various Italian national agencies and regional meteorological services. BOLAM and MOLOCH differ in their dynamical core, including a different choice for their vertical coordinate sets, and by the fact that BOLAM includes a parameterization for deep convection, based on a modified version of the Kain-Fritsch scheme (Kain, 2004). In MOLOCH deep convection is explicitly simulated and a simple shallow convection scheme is applied. BOLAM (horizontal resolution 11 km, 50 vertical levels) is run over a European domain and it is mainly employed to provide lateral boundary conditions for the inner grid (horizontal resolution 2.3 km and 54 vertical levels) of MOLOCH (Figure 1) at 1-hour intervals. This intermediate nesting step has proved to be reliable and economical in bridging the gap between the coarse-resolution global model fields (0.25°/6-hourly ECMWF analysis data) and the high-resolution forecasts (Buzzi et al., 2014). Therefore only a brief description of the MOLOCH model is provided here. For a description of BOLAM refer to Buzzi et al. (2003), Malguzzi et al. (2006) and Davolio et al. (2013).

MOLOCH is a non–hydrostatic, fully compressible, convection-permitting model (Malguzzi et al., 2006; Buzzi et al., 2014). It integrates the set of atmospheric equations with 12 prognostic variables — pressure, absolute temperature, specific humidity, horizontal and vertical components of velocity, turbulent kinetic energy and five water species (cloud water, cloud ice, rain, graupel and snow) — represented on the latitude–longitude, rotated Arakawa C-grid. It employs a hybrid

terrain-following vertical coordinate, depending on air density and smoothing to horizontal surfaces at higher altitudes. Time integration is based on an implicit scheme for the vertical propagation of sound waves, while explicit time-splitting schemes are implemented for integration of the remaining terms of the equations of motion. Three-dimensional advection is computed using the Eulerian weighted average flux scheme (Billet and Toro, 1997). The physical parameterisation schemes are common between the two models. The microphysical scheme is based on the parameterisation proposed by Drofa and Malguzzi (2004). Atmospheric radiation is computed with a combined application of the Ritter and Geleyn (1992) scheme and the ECMWF scheme (Morcrette et al., 2008). The turbulence scheme is based on a turbulent kinetic energy – mixing length (*E-l*) order 1.5 closure theory (Zampieri et al., 2005). The soil model uses seven layers and it takes into account the observed geographical distribution of different soil types and soil physical parameters. For a more detailed description of MOLOCH refer to Buzzi et al. (2014).

In the present study, the NWP system was applied to six case studies (Table 1). First, a thorough verification of the simulations was performed in order to verify that the model correctly reproduced the main dynamical features of each event. Model simulations were compared with observations, such as the dense ground-based station networks (which observed near-surface temperature, wind, humidity and precipitation), radiosoundings and operational wind profilers over northern Italy, in order to assess the mesoscale features. The large-scale dynamics was compared against ECMWF analyses. No special observations, except for some additional soundings, were available over the NEI area for IOP18 and IOP19 events. However, it is worth mentioning that the unprecedented collaboration fostered by the HyMeX-SOP1 among research institutions and regional meteorological centres and agencies (Davolio et al., 2015) allowed a fruitful collaboration and sharing of observation database (national radar composite and raingauge network, among others). For the sake of brevity, only the comparisons concerning the total precipitation are presented.

For each case study, different initialization times for BOLAM and for MOLOCH nesting were tested and the best simulation was chosen as the “control run” to investigate each episode. We made

this choice to ensure that the simulation is as close to reality as possible, in terms of location, intensity and evolution of the precipitation, as well as of triggering and organization of the precipitating systems, so as to investigate the physical mechanisms rather than the skill of operational forecasting.

3. Heavy precipitation events over NEI

A brief description of the selected events, listed in Table 1, is provided here, based on model simulations and comparisons against available observations. The model simulations are used to investigate the physical mechanisms responsible for the precipitation events in Section 4.

From a preliminary analysis, it turned out that all the selected events were driven by similar large-scale conditions (Figure 2), i.e. a synoptic scale trough extended over the Mediterranean and the low-level flow was southerly, coming from the Adriatic Sea. Moreover, during the initial stage of the events the mesoscale flow features were also similar. The pre-existing cold air over the plain of NEI enhanced the low-level blocking caused by the incoming flow damming up against the Alps (Di Muzio, 2014). This produced a strong deflection (flow around) of the southerly flow by the Alps, causing a barrier wind (Buzzi, 2004). This deflection produced north-easterly wind at the foot of the Alps, initially preventing the warm air from advancing inland towards the mountains.

The analysis of the events also showed that, after the initial stage, different mesoscale evolutions were responsible for the different precipitation patterns already mentioned (the low-level flow evolution is thoroughly analysed in Section 4.2). This led us to separate the events into two main categories. Hereafter we refer to “Alpine” events that were characterised by heavy, widespread rainfall over the Alpine area, associated with uplift of the southerly low-level flow over the orographic barrier, which represents the most frequent case in such situations. In addition to IOP19, two recent heavy-precipitation episodes affecting the Alps were also analysed (Table 1). In contrast, we refer to “Upstream” events that were characterised by intense and almost stationary convective precipitation over the plain upstream of the orography, associated with persisting low-level

blocking of the impinging southerly flow. In addition to IOP18, two Upstream events were selected among those discussed in Barbi et al. (2012). However, since the interest is placed on orographically modified flow, we have not considered the other two cases included in the study of Barbi et al. (2012), which were similar in terms of precipitation distribution but characterised by north-easterly Bora wind instead of barrier-type wind.

Generally, simulated rainfall showed a better agreement with the observations for the Alpine (Figures 3 and 4 (a), (b), (c)) rather than the Upstream events (Figures 3 and 4 (d), (e), (f)). The direct orographic uplift, which represents a fairly large-scale forcing, is probably better simulated by the model than the local triggering of convection, and may thus account for the larger degree of predictability.

3.1 IOP19

By 4 November 2012, an upper-level trough extended from the Scandinavian Peninsula to the Atlantic Ocean, with a surface pressure minimum close to Ireland. The Mediterranean was affected by intense south-westerly flow in the middle troposphere, while a warm conveyor belt ahead of the cold front advected warm air towards the Italian peninsula (Ferretti et al., 2014). At the surface, the development of a shallow cyclone over the Gulf of Lion, progressively moving towards northern Italy, favoured intense low-level warm and moist southerly flow over the Adriatic Sea. The synoptic pattern (Figure 2(a)) evolved slowly during 4 and 5 November, due to the presence of a pressure ridge over eastern Europe, and was associated with intense precipitation over NEI (Figure 3(a)), especially in the areas close to the Slovenian border, where a maximum of 370 mm in about 24 hours was observed. While the precipitation was very weak over the plain, intense rainfall, exceeding 200 mm in 24 hours, was recorded over a wide area of the Alps. However, only a few lightning strikes were detected indicating that the precipitation was mainly stratiform/orographic in nature. This is also supported by low Convective Available Potential Energy (CAPE) values, and moderate vertical motion was only attained during the final phase of the event, as indicated by both

model simulations and data from the Campoformido (Udine) radiosounding (location in Figure 1). MOLOCH correctly simulates the rainfall distribution (Figure 4(a)), although it slightly underestimates the orographic rainfall. Also, the hourly rainfall evolution is in good agreement with radar estimates (not shown), with the heaviest precipitation occurring in the evening over the north-easternmost sector of NEI Alps. The model simulates a slightly faster passage of the cold front over the area, thus sweeping away the precipitation system about two hours earlier than observed.

On the mesoscale, it is worth mentioning that in the initial phase of the event, cold air was present over the plain (average θ_e was 313 K close to the ground), and a barrier wind developed ahead of the Alps, due to the westward deflection of the southerly wind coming from the sea, as predicted by MOLOCH and confirmed by wind measurements taken just inland of the Adriatic coast (not shown). The inflow from the sea was initially forced to rise over the cold air. Later, while increasing its intensity, the southerly flow was characterised by a gradual transition from flow-around to flow-over conditions, associated with the removal of the cold air at the base of the orography. The uplift was then directly forced by the passage over the Alps, where most of the precipitation occurred (Figure 3(a)).

3.2 Piancavallo 2012

Between 10 and 11 November 2012, just a few days after the end of the SOP1, a trough deepened over the Iberian Peninsula (Figure 2(b)), reaching Northern Africa and activating intense warm and moist south-westerly flow over the central Mediterranean. The eastward evolution of the trough was very slow and a cut-off low eventually formed over Spain. The low-level moist flow over the Adriatic Sea produced heavy rainfall (almost 400 mm in 24 hours) over the Pre-Alpine area (Figure 3(b)), between Veneto and FVG regions, while precipitation was light over the plain. MOLOCH correctly simulates the orographic precipitation (Figure 4(b)) although the maximum accumulation is underestimated by about 20% (310 mm instead of 390 in 24 hours at Piancavallo, over the FVG Alps; Table 1). Similar to IOP19 event, the Sirocco wind, initially deflected ahead of the Alpine

barrier, progressively penetrated inland, gently rising over the Alps. Again, this wind pattern is confirmed by SODAR wind profile measurements (not shown). During the most intense phase of the event, MOLOCH simulates vertical velocities of a few m s^{-1} within the precipitation system, indicating the probable development of embedded convection.

3.3 Vicenza 2010

This event was a long-lasting episode of intense precipitation, leading to a major river flood in the city of Vicenza (location in Figure 1). After weak rainfall during the morning of 31 October 2010, moderate to heavy precipitation developed over the Pre-Alpine area, persisting into 1 November, while only weak rainfall affected the plain. As in the previous cases, rainfall was associated with a deep trough over the Mediterranean basin (Figure 2(c)), evolving into a cut-off low over the Gulf of Lion in the final phase. A reinforcing ridge over eastern Europe slowed the eastward progression of the trough, thus favouring the stationarity of the intense low-level Sirocco wind over the Adriatic Sea and the persistence of precipitation. The location of intense rainfall was strictly correlated with orographic features along a WSW-ENE direction over the Pre-Alps (Figure 3(c)) and the pattern did not change throughout 31 October and 1 November. The most intense phase of the event was characterised by rainfall reaching 460 mm in 48 hours in Veneto and about 600 mm in 48 hours in FVG. However, considering the whole 72-hour period of rainfall, more than 700 mm were recorded in FVG and more than 500 mm in several stations in the Veneto region. As shown in Figure 4(c) MOLOCH correctly simulates the precipitation pattern, displaying intense rainfall over the Alps. The hourly evolution (not shown) is properly simulated, with increasing rain rate in the morning of 1 November, possibly associated with embedded convective activity, and rainfall progressively weakening in the afternoon, eventually becoming scattered. Also in this case, the initially weak low-level south-easterly flow from the Adriatic Sea was blocked and deflected as a barrier wind, but as it increased in intensity, it was able to flow over the Alps. This feature is confirmed by

SODAR wind profile observations (Figure 5(a)) taken in Concordia Sagittaria close the Adriatic coast (location in Figure 1).

3.4 IOP18

On the morning of 31 October 2012, a secondary cyclone developed over Spain, embedded in a larger cyclonic circulation centred north of the British Isles. This low-pressure system moved eastward over the Gulf of Lion reaching Corsica in the afternoon (Figure 2(d)) and inducing low-level south-easterly moist unstable flow over the Adriatic area, impinging on the Alps, and south-westerly flow aloft. In contrast to the previous events, here the low-level intense currents over the Adriatic basin were not able to pass over the Alps during the whole event and the persisting convergence line between the Sirocco wind and the barrier wind focused the convective activity over the Veneto plain, just north of the Po river outlet. Radar images (not shown) revealed that initially the rainfall was produced in the early afternoon of 31 October by convective systems triggered over the Adriatic Sea and then advected inland over the Po Valley. This phase of the event is reproduced with some delay in MOLOCH, which simulates intense rainfall over the plain only after 1700 UTC. Later in the evening of 31 October, almost stationary convection developed over the plain, related to the convergence line. Although the complete picture of simulated rainfall is affected by a significant error in the location (Figure 4(d)), the simulation captures correctly the dynamical evolution of the low-level flow and of the convergence line, as well as the total rainfall. Therefore, the model reproduces the convective activity and its stationarity, but slightly later than observed. In less than 12 hours, intense precipitation exceeding 120 mm affected a restricted area of NEI (Figure 3(d)). For some raingauge stations the return period of the event was calculated to be longer than 50 years. However, the rapid eastward progression of the cyclone moved the precipitation away. Observation revealed that wind gusts over the Adriatic exceeded 80 km h^{-1} (not shown) and a major storm surge affected the NEI coast.

3.5 Marghera 2007

This event, thoroughly described and investigated in Davolio et al. (2009b) and Rossa et al. (2010), was the most intense rainfall episode that occurred during the operational period of the MAP-DPHASE project (Rotach et al., 2009). It was responsible for a severe, although localised, flood over a flat area near Venice (location in Figure 1) on 26 September 2007. It was associated with a stationary mesoscale convective system (MCS) that developed west of the Venice lagoon (Barbi et al., 2012), and took a V-shape in infrared satellite imagery (Setvák et al., 2013). More than 320 mm fell in less than 12 hours (Figure 3(e)), of which more than 240 mm fell in only 3 hours. An upper-level trough, deepening over France and the Mediterranean while approaching the western Alps (Figure 2(e)), favoured orographic cyclogenesis over the Gulf of Genoa and produced a south-westerly diffluent flow over NEI. The orographically-induced cyclone enhanced the south-easterly low-level jet over the Adriatic Sea, which was deflected in front of the Alpine barrier. The MCS was triggered along the convergence line between the Sirocco wind and the barrier wind. MOLOCH simulates scattered convective activity in the early morning, turning into organised convection able to produce large rain rate up to 180 mm h^{-1} close to the Venice lagoon (Figure 4(e)). Low-level convergence, stationary convection, as well as the orientation of the V-shape structure of the MCS are correctly simulated. Differences between the structure of the observed and forecast rainfall fields remain within the expected variability for this particular event, as discussed in Davolio et al. (2009). Finally, the persistence of blocked-flow conditions and of the barrier wind over the NEI plain is confirmed by SODAR observations (Figure 5(b)) taken close to the city of Padua (location in Figure 1).

3.6 Mira 2009

On 16 September 2009 the synoptic circulation was characterised by a cyclonic disturbance over the western Mediterranean basin (Figure 2(f)) and south-westerly flow in the middle troposphere over NEI. The cut-off cyclone centred between Spain and France induced moist south-easterly flow

in the lower levels over the Adriatic Sea. Again, the interaction between the north-easterly barrier wind in front of the Alps and the Sirocco wind produced a convergence pattern able to trigger convective activity over the Veneto plain, close to the Venice lagoon. In the early morning convective cells moved from the Adriatic Sea towards the Pre-Alpine ridge and later became more stationary, regenerating along the coastal area. Around 1200 UTC, a stationary MCS developed producing intense rainfall. This evolution explains the precipitation pattern shown in Figure 3(f) characterised by a main maximum of about 180 mm in 24 hours close to the coast and weaker localised maxima over the Pre-Alps. The MOLOCH simulation of this event is not completely satisfactory (Figure 4(f)), but reproduces the most intense phase of stationary convection around 1200 UTC, which is the most relevant aspect for this study. Indeed, a rainfall maximum is simulated over the plain, although displaced south-westward and less intense of the maximum over the orography.

4. Physical mechanisms

4.1 Theoretical framework

The cases summarised in Section 3 are characterised by the interaction of moist and warm flow with a mountain ridge. Before presenting a detailed investigation of the events in terms of physical mechanisms and numerical parameters, a brief review of the main scientific achievements in the field of orographically modified flow and orographic precipitation is provided, highlighting the framework and motivation of the present study.

Idealised studies of stably-stratified dry flows impinging on a mountain ridge revealed the Froude number ($Fr = U/(N \cdot h)$ where U is a measure of the wind speed, h is a typical height of the mountain and N is the static stability) as the main parameter able to discriminate between a "flow-over" regime, when the flow passes over the ridge without being significantly deflected ($Fr > 1$), and a "flow-around" regime, when the flow is blocked in the lower layers and deflected by the ridge ($Fr < 1$) (Smolarkievicz and Rotunno, 1990). Pierrehumbert and Wyman (1985) evaluated the upstream

influence of the orography and showed that upstream blocking and flow diversion in a rotating atmosphere is strictly connected with barrier winds that are generated as a consequence of the damming of low-level stable air. This aspect is particularly relevant as a theoretical support for the observed phenomenon of barrier wind over NEI described in Section 3.

The introduction of moisture, which modifies the "effective" static stability N of the air at saturation and hence the dynamical response to orographic forcing, depending on when and where condensation occurs, may favour the flow-over regime (e. g. Miglietta and Buzzi, 2004). In the last decade, attention has been mainly focussed on conditionally unstable moist flow and on regimes of convection propagation in presence of orography, pointing out the limited applicability of Fr in such conditions. Chen and Lin (2005) and Miglietta and Rotunno (2009) found that Fr taken alone is unsuitable to explain the precipitation distribution in a convective environment. Thus, Miglietta and Rotunno (2009, 2010) introduced several non-dimensional parameters to account for orographic triggering of convection in conditionally unstable flow and subsequent interactions between the environmental flow and the convective cold pool. In particular, the parameter h_m/LFC, namely the ratio between ridge height (h_m) and the altitude of the level of free convection (LFC), was suggested to quantify the likelihood that orographic lifting is sufficient to initiate convection.

In addition to idealised simulations, important results came also from case studies analyses, mostly fostered by field campaigns (Rotunno and Houze, 2007). Buzzi and Foschini (2000) and Rotunno and Ferretti (2001, 2003) identified important aspects of Alpine heavy rainfall episodes, both at the synoptic- and meso-scale, like the presence of low-level jets and along-ridge gradients of relative humidity able to influence flow ascent through condensation and latent heating. More recently, the dynamics of a low-level moist jet interacting with a complex-shaped ridge has been studied in Nuissier et al. (2008) and Bresson et al. (2009, 2012). They showed that the location of convection triggering and the characteristics of the MCS, in terms of stationarity and accumulated rainfall, depend on different environmental parameters, such as ridge shape, low-level horizontal wind and humidity profiles, CAPE and upstream cold pool features. Finally, the characterisation of the

environment associated with heavy precipitation, in particular concerning the thermodynamic properties of the low-level jet, has been also explored through a climatological approach (Rudari et al., 2004; Ricard et al., 2012).

In analogy with the above-mentioned findings, we tried to apply the theoretical results to the observed cases, in order to identify parameters able to describe the different behaviour observed for Upstream and Alpine events. However, it is worth bearing in mind that in real case studies the environment is more complex than in idealized experiments.

4.2 Overview of the dynamical evolution

The dynamical characteristics of the flow interacting with the Alpine orography are preliminarily investigated computing the moist Fr using a vertical profile obtained as an average over an area of about 50 x 50 km centred in 45 °N – 13 °E (shown in Figure 7). This area, located in the middle of the northern Adriatic Sea, is chosen to sample the mesoscale incoming flow upstream of the orography. Fr is computed every three hours, starting from the onset of impinging flow and until the flow in the area can be considered not yet perturbed by the interaction with the orography or by the occurrence of intense rainfall. However, several drawbacks emerge preventing us from the possibility to identify clearly the two separate classes of events using Fr. In fact, in addition to the known difficulties arising in Fr computation in the case of conditionally unstable flow (Miglietta and Rotunno, 2009), even for almost stratified flow as in the Alpine events results do not completely meet expectations. Fr is computed using h = 2000 m for orography height, averaging the meridional component of the wind over the model levels up to this height, and evaluating the flow stability as suggested in Barrett et al. (2014):

$$N^2 = \frac{g}{\theta_t}\frac{\theta_t - \theta_b}{h}$$

where g = 9.81 m s^{-2} while θ_b and θ_t are respectively virtual potential temperature at the lowest model level and at the model level corresponding to about 2000 m. Fr values barely exceed one

(Figure 6), as it would be expected in case of flow-over regime. However, a more detailed analysis reveals a strong horizontal gradient of Fr values across the Adriatic basin for the Alpine events, and thus a strong sensitivity to the selected area of computation. In particular, Fr values much larger than unity are found on the eastern side of the Adriatic basin, while values lower than unity characterise the flow close to the Italian coast. Thus, instead of considering the absolute Fr value, whose computation may be somewhat arbitrary, the attention is focused on its evolution in time. Figure 6 shows that for all the three Alpine events Fr steadily and substantially increases during the event. This is consistent with blocked-flow and barrier wind conditions at the beginning of the event and a gradual change towards a flow-over regime, starting from the easternmost part of the Alps, as simulated by MOLOCH and confirmed by available observations (soundings and wind profilers, e.g. in Figure 5(a)). On the other hand, for the Upstream events and especially for M2007 and M2009 cases, Fr values remain low, hardly exceeding 0.6. The exceptionally strong wind attained during IOP18 is responsible for a temporary increase of Fr, although not higher than 0.8. However, in this latter case, the low-level wind is also steered by the mesoscale cyclonic circulation that forces its rotation from the Adriatic Sea into the Po Valley, thus favouring the blocking effect of the Alps. It is also worth noting that Fr for the Alpine events is generally larger than the value obtained for the Upstream events, thus suggesting a different flow regime. Therefore, although the absolute value of Fr does not provide critical information, relative values between different events seem to be able to describe different dynamical characteristics of the analysed events.

Keeping in mind these results and the theoretical background briefly described in Section 4.1, the analysis is focussed on two different phases of the events: (i) the triggering phase, being the initial period characterised by the possible development of convective cells and precipitation initiation; (ii) the precipitation phase, when the precipitating system is well developed. For the sake of brevity and clarity, most of the results are presented only for two events, representative of the two categories: V2010 for Alpine events and M2007 for Upstream events.

4.3 The triggering phase

During the initial phase of both events, the low-level wind field (Figures 7 (a), (b)) displays a similar pattern, characterised by blocked flow upstream of the Alps, possibly enhanced by the presence of pre-existing cold air (Pierrehumbert and Wyman, 1985), producing a north-easterly barrier wind over the NEI plain and over the Po Valley. The convergence between the barrier wind and the Sirocco wind from the Adriatic Sea clearly show up in Figure 7 as a narrow zone of low wind speed. However, the consequence of this convergence is quite different, as shown by the cross sections drawn along the direction of the impinging flow. On one hand, for V2010 case (Figure 8(a)) the moist south-easterly flow gently rises over the cold layer located at the foot of the Alps where the barrier wind is blowing, before being further lifted over the orography. No precipitation is associated with the uplift during this phase. On the other hand, in M2007 event (Figure 8(b)) convection is triggered in correspondence with the ascent over the barrier wind cold layer and intense precipitation is suddenly produced.

This different behaviour has a critical impact on the following dynamical evolution, when the intensity of the impinging flow increases in response to the approaching synoptic disturbance. As shown in Figures 7(c), in V2010 southerly flow progressively penetrates into the plain, the cold barrier wind layer disappears and the flow eventually passes over the Alps. All over the eastern Alps the 10-m wind field displays a clear flow-over pattern in response to increasing wind speed, while the flow stability remains nearly constant. Consequently, precipitation affects mountainous areas where uplift and condensation occur. The cross section (Figure 8(c)) also indicates some small-scale and intense vertical motions over the orography, possibly due to embedded convective activity that locally enhances rainfall intensity.

Conversely, the convergence pattern along the coastal area persists in M2007 (Figure 7(d)). The blocking conditions persist, consistent with the result of the Fr analyses, the low-level flow does not penetrate inland and deep convection intensifies (Figure 8(d)), fed by moist and warm air from the Adriatic Sea. This resembles the blocked-flow condition considered as the most favourable to heavy

rainfall rates in the idealised experiments shown in Miglietta and Rotunno (2014) and in Davolio et al. (2009a), characterised by a convective cold pool propagation nearly countered by the environmental wind. The role of the evaporative cold pool is further discussed in Section 4.5.

Now that the general physical mechanisms have been described, a more detailed thermodynamic analysis concerning the initial triggering phase of the events is performed. First, vertical thermodynamic profiles are analysed (Figures 9(a), (b)). Profiles are not computed for a single grid point but as an average over an area of about 15 x 15 km over the northern Adriatic Sea, almost contained in the area used for computing Fr. Using an upstream area gives a better sampling of undisturbed flow characteristics before its interaction with the orography and with the cold pool producing uplift and possibly triggering convection. Profiles are computed for the initial phase of the events, when convection is possibly being triggered but intense precipitation has not started yet. These profiles allow for the evaluation of the LFC height and CAPE (using the most unstable parcel) and several indices related to stability (Tables 2 and 3). Similarly, vertical profiles over the NEI plain, together with the analysis of cross sections similar to those presented in Figure 8, provide the estimate of h_b as the top of the layer characterised by stable stratification and north-easterly wind. This layer is found to be quite shallow, with its depth always being lower than 800 m.

Although it is possible to identify an LFC located at a relatively high elevation, around 1000 meters, the profile for V2010 (Figure 9(a)) shows a nearly neutral moist vertical stratification of the air mass, even stable in the lower layers and with very low CAPE values (below 50 J kg^{-1}). This is a common characteristic among the Alpine events, with the LFC being even higher in IOP19. The wind veers by about 45 degrees over the lowest 2 km. The moisture content is already high at the beginning of the simulation and the air column becomes saturated quite quickly during the first day of the event (not shown), without relevant changes in stability properties. On the other hand, for M2007 (Figure 9(b)) and similarly for M2009 (not shown) the atmosphere is conditionally unstable, close to saturation in the lowest layers and much drier above 850 hPa where the wind direction

abruptly changes from south-easterly to south-westerly. The LFC is fairly low, being located below 500 m and the value of CAPE is relevant, greater than 1000 J kg^{-1}. It is worth mentioning that the vertical profile for IOP18 (not shown) is also characterised by a low LFC. However, moisture is higher and more uniform all over the troposphere and CAPE is lower and mainly concentrated in the lower layers, as usually observed for autumn events with respect to late summer cases.

The described behaviour is also in agreement with positive values of the Lifted Index (Galway, 1956) (LI > 2.2 K, in Table 2) found for the Alpine events, which indicate stable conditions during the initial phase of the event. For the Upstream events (Table 3) potential instability is instead present. This is especially true for M2007 and M2009 events, which have a negative LI, but also for IOP18, even if the LI indicates nearly neutral conditions (0.5 K). Indeed, referring to a climatological statistical analysis of convective events over the FVG area (Manzato, 2003) a LI of +0.64 K represents the discriminant value to classify convection development in the FVG plain.

While it is evident that deep convection cannot develop in the initial stage of the Alpine events, the Upstream events deserve a further analysis of the triggering phase. Among the relevant parameters modulating rainfall rate and location for a conditionally unstable flow over a ridge, Miglietta and Rotunno (2009) suggested to use the ratio of mountain height to the level of free convection (h_m/LFC). This parameter evaluates whether the uplift forced by the mountain is sufficient to allow air parcels to reach their LFC and thus to trigger convection. In the present analysis the same idea is adopted, but considering the cold layer with barrier wind, instead of the mountain, as the "obstacle" providing the initial uplift forcing. A similar approach was used by Mazòn and Pino (2013) in their analysis of convective cloud bands developing near the Mediterranean coasts. In other words, this cold layer located upstream of the orography, and characterised by the barrier wind, acts as an "effective mountain" (Lin et al., 2005) of height h_b.

Values of h_b/LFC computed for the three Upstream events during the triggering phase are close to or greater than unity, consistent with the fact that convection is triggered where the impinging and barrier flows meet. For IOP18, besides the main rainfall episode that occurs in the late evening

(associated with the highest value of h_b/LFC), an interesting convective phase in the morning is also considered, when shallow convective activity developed over the Adriatic Sea in correspondence with the aforementioned convergence line. Also in this case h_b/LFC is close to unity. However, during IOP18, convection is triggered but does not develop into deep convection. Instead, for M2007 and M2009 events, high values of CAPE indicate favourable conditions for vigorous convective vertical motions and heavy rainfall.

Another clear indication concerning the type of event can be obtained by considering the buoyancy of air parcels displaced vertically from multiple levels (Davolio et al., 2009a; Buzzi et al., 2014). At each model level, the virtual temperature of an air parcel adiabatically raised by a given displacement is computed and compared with the virtual temperature of the environment at the new altitude. Since early stages of convection are analysed, computation assumes the loading of condensed water (reversible uplift), considers the occurrence of precipitation negligible, and entropy conservation of a mixture of air/vapour/cloud water. The virtual temperature difference between the parcel and the environment, is used to calculate the buoyancy as follows:

$$B = g\frac{T_v^{par} - T_v^{env}}{T_v^{env}}$$

Buoyancy is computed as a function of the height of the parcel, thus providing a buoyancy profile relative to more parcels. Figure 10 shows the results for a vertical lift of 500 metres. Similar results hold for slightly different vertical displacements (consistent with the height of the leading edge of the barrier-wind cold layer), small enough to assume that condensed water is still retained by the lifted parcel. The Upstream convective cases are characterised by positive buoyancy, and thus instability to small vertical displacements in the lowest atmospheric layer of depth of roughly 1000 metres. The vertical profile of buoyancy for IOP18 is characterised by larger values close to the ground, progressively decreasing aloft. This is consistent with thermodynamic profiles close to saturation, unstable in the lower layers and almost neutral above, with moderate CAPE values. Conversely, M2007 and M2009 thermodynamic profiles (Figure 9(b)) indicate increasing relative

humidity with height in the first 1500 metres, characterised by a lapse rate close to the dry adiabatic. Thus buoyancy shows that the most unstable parcels are located at around 500 metres above the surface and not near the ground. Conversely, buoyancy presents negative values for the Alpine events, indicating overall stable conditions. The buoyancy profile for IOP19 is slightly different between 1000 and 2000 m, but still representative of stability to vertical displacements.

In summary, the thermodynamic profile of the impinging southerly flow, which is forced to rise over the cold stable layer located over the plain upstream of the orography, determines the different behaviour observed in the two classes of event. h_b/LFC reveals the possible triggering of convection during the first phase of the events, in case of conditional instability. Also LI turns out to be important because it indicates a necessary condition for potential instability in order to realise vigorous convective activity. Once convection is initiated, its intensity is related to CAPE.

4.4 Precipitation phase: Alpine events

As previously described, if convection is not triggered in correspondence with convergence and uplift, the south-easterly flow is able to progressively penetrate towards the Alps, replacing the pre-existing cold air ahead of the orography. Consistently, a gradual transition from blocked-flow to flow-over conditions is observed. However, model simulations (see for example the cross section in Figure 8(c)), as well as rainfall and remote sensing observations, reveal that convective activity can be embedded in the orographic precipitation, at least in the most intense phase of the events. This is a quite typical characteristic of heavy-precipitation events over north-eastern Alps, usually referred to as flux precipitation (Manzato, 2007), that deserves further investigation.

As presented in Section 4.2 for the Alpine episodes, variation of Fr describes the transition to a more pronounced flow-over conditions during the event. Moreover, an analysis of the thermodynamic vertical profiles upstream of the orography reveals that the impinging flow becomes progressively more unstable, and during the precipitation phase slightly unstable conditions are attained. Therefore, the parameter h_m/LFC becomes suitable to explain the possible

occurrence of convective activity. In Figure 11, the evolution in time of h_m/LFC is plotted for the Alpine events. Values of h_m/LFC increase progressively, becoming close to or larger than unity in correspondence to the initiation of intense precipitation. This confirms that the uplift forced by the Alps is able to trigger convective activity, since the air parcels are forced to rise above the level of free convection. Moreover, low CAPE values are consistent with the presence of weak to moderate convection, acting to locally enhance rainfall rates. V2010, besides being the longest lasting event, is also characterised by a more pronounced potential for convection development (Figure 11). It is worth noting that rainfall enhancement over the windward slopes of the orography can be also due to small-scale turbulence and microphysical processes (i.e. seeder-feeder mechanism), as described for the western Alps for unblocked low-level flow (Rotunno and Houze, 2007).

4.5 Precipitation phase and the role of the cold pool in the Upstream events

When convection initiates resulting from uplift over the cold layer, the southerly low-level moist flow is intercepted by the convergence line and hardly reaches the Alps. The convergence line persists almost in the same position for several hours. Thus, although the direct orographic forcing is not the main lifting mechanism, the Alps are responsible for the persisting blocked-flow conditions, as displayed by the Fr analysis in Section 4.2. This can account for the stationarity of the convective systems. However, the formation of evaporative cold pools is crucial in determining organisation and propagation properties of convective systems (Emanuel, 1994). In the present cases, cold-air layer formation precedes the convection onset; however, once convection has developed, cold pools can be reinforced by evaporative cooling and can thus interact with the upstream flow, forcing the low-level flow up and over its head (Bresson et al. 2012; Miglietta and Rotunno 2009). In order to explore this aspect, additional MOLOCH simulations were performed for the three Upstream events. These experiments were similar to their respective control runs, except that the contribution to the temperature tendency due to evaporation or sublimation of precipitation was removed in the microphysics parameterisation scheme.

Figure 12 presents the results for M2007. The accumulated rainfall (Figure 12(a)) indicates that, in this simulation, the convective system persists over the plain of the Veneto region, just inland the Adriatic coast. With respect to the control simulation (Figure 4(e)), the precipitation maximum is shifted about 20 km to the northeast and displays a different orientation, although the intensity does not differ markedly (370 mm/12h). The lack of the precipitation band over the sea, parallel to the coast, reveals the main difference between the two simulations. The triggering phase is very similar, but during the mature stage the evaporative cooling actually reinforces the cold pool. Thus, in the control simulation (Figure 8(d)) the convective system slightly propagates against the low-level environmental flow blowing from the Adriatic Sea, as can be seen comparing Figures 8 (b) and (d). Conversely, without the cooling effect of the evaporation beneath the convective system, the low-level atmosphere upstream of the Alps is warmer and the signature of the cold pool much less evident (Figure 12 (b)). The convergence line, the convective updraft and hence the precipitation system remain over land, north of the coastline but still upstream of the orography.

It is worth mentioning that additional experiments were performed in order to evaluate the respective impact on the cooling of evaporation and sublimation of the precipitation. It turned out that the main contribution comes from rainfall evaporation, since the sublimation of ice microphysical hydrometeors does not change the results significantly, with respect to the control simulations.

Similar results were obtained for the other two events. Therefore, such experiments indicate that although evaporation/sublimation of precipitation is able to influence to some extent propagation and hence position of convection, it does not determine the stationarity of the systems. Upstream convergence due to persisting blocked-flow conditions is the primary mechanism producing that stationarity.

Following Miglietta and Rotunno (2009), the convective system is triggered and continuously regenerated as expected when h_m/LFC is larger than one (Table 3). Moreover, their idealised simulations of conditionally unstable flow past a mountain ridge showed that stationary convection

occurs when the advective time scale τ_a is longer than the convective time scale τ_c. Although the applicability of theoretical results is not always straightforward for real events (Miglietta and Rotunno 2012, Bresson et al. 2012) an estimation of the proposed non-dimensional parameters is presented in the following. Table 3 lists the relevant parameters, evaluated for upstream conditions: Downdraft Convective Available Potential Energy (DCAPE), $CAPE^{1/2}$ / U, which is almost proportional to τ_a / τ_c, $DCAPE^{1/2}$ / U, representing a measure of cold-pool propagation and N LFC / U, which evaluates the impact of cold pool propagation on the upstream flow.

The results for M2007 and M2009 are very similar and the location of the precipitation seems to be correlated with the theoretical results. Moderate wind speed and large instability (large values of $CAPE^{1/2}$ / U) are consistent with a stationary convective system upstream of the mountain ridge, since there is enough time for evaporative reinforcement of the cold pool and redevelopment of convective cells over the same area ($\tau_a > \tau_c$). Moreover, the intensity of downdraft indicates the possibility to have a slight propagation of the cold pool against the low-level environmental flow for M2007, as actually observed. For IOP18 the comparison is even more difficult, since it is a low-CAPE case with very strong wind. Although parameters suggest the triggering of convection, it seems that intense wind speed does not create favourable conditions for long-lasting stationary convection, as instead occurs during M2007 and M2009. It can be argued that in this case other mechanisms could have contributed to the organisation of the convective system. In particular, cyclonic mesoscale forcing could have played a role during the first part of the precipitation phase by advecting convective cells from the Adriatic Sea towards the convergence line and later on favouring the deflection of the low-level flow. The strong vertical shear characterised by a variation of the along-ridge component of the flow could have also affected the convective system evolution (Miglietta and Rotunno, 2014).

5. Conclusions

The present study was motivated by observations made during the HyMeX-SOP1 campaign, which documented two heavy-precipitation episodes (IOP18 and IOP19) characterised by similar synoptic situations and initial mesoscale conditions of blocked-flow impinging on the Alpine barrier but with a completely different dynamical evolution, leading to different precipitation patterns. During IOP18, blocked-flow conditions persisted and the low-level south-easterly flow came from the Adriatic Sea and was then deflected in front of the orography as a north-easterly barrier wind, creating a convergence line upstream of the orography, where convection was triggered. Heavy precipitation affected the plain area of NEI well upstream of the orography. Conversely, during IOP19 the south-easterly flow was blocked by the Alps only in the initial phase, but then progressively penetrated inland reaching the Alpine ridge, consistent with flow-over conditions. This situation produced intense rainfall over the orography. This evidence prompted a survey and an analysis of other similar cases, in order to identify common mechanisms leading to two different precipitation patterns over NEI.

Notwithstanding the peculiar features and the complexity of each analysed event, the present study, based on high-resolution NWP model simulations validated and supported by observations, shows clearly that the two different rainfall patterns belong to two different “regimes” of precipitation event that often affect the NEI area, as summarised in the schematic diagram of Figure 13. For all the events, the low-level south-easterly flow (Sirocco wind) is initially blocked by the Alps and deflected as an easterly/north-easterly barrier wind over the NEI plain. The presence of pre-existing cold air over the NEI plain, resulting from nocturnal radiative cooling, enhances the low-level blocking. As the synoptic disturbance progresses, the low-level wind intensifies and, depending on the thermodynamic vertical profile of the impinging flow, convective activity may be triggered in the initial phase. In the Upstream events (Figure 13(a)), convection initiates well upstream of the orography where the incoming flow is forced to rise over the cold layer characterised by the barrier wind. Blocked-flow conditions persist and the convergence line between the Sirocco wind and the barrier wind triggers further convection. The cold pool is even reinforced by evaporative cooling of

the convective precipitation, but specific model simulations have proved that the stationarity of the convective system is determined by the persisting blocked-flow conditions by the Alps, confirmed by low Fr values. The low-level flow from the Adriatic Sea is intercepted and thus it feeds the convection and does not reach the orography. Therefore, precipitation affects the NEI plain or even the coastal area, far upstream from the Alps.

In the Alpine events (Figure 13(b)) convection does not develop as a result of the forced uplift over the cold air. Flow-over conditions progressively become established and the low-level flow coming from the Adriatic Sea reaches the Alps, while the cold air ahead of the orography is removed. This is also supported by progressively increasing values of Fr. The barrier wind disappears and the orographically forced uplift of the impinging flow produces intense precipitation over the Alps.

Therefore, rainfall location turns out to be the consequence of different dynamical behaviour of the flow impinging on the orography and its thermodynamics characteristics are critical for the triggering of convective activity due to uplift over the barrier wind cold layer. If the profile is unstable and the LFC is located at low altitude, this uplift is strong enough to trigger convection over the plain upstream. Indices such as LI, CAPE, TLIFT and h_b/LFC proved able to take into account the mechanisms responsible for the different phenomena observed during the triggering phase.

The results obtained for the convective events are in agreement with theoretical studies of conditionally unstable flow over orography. The value of h_m/LFC much greater than unity indicates occurrence of convection upstream of the orography and the other parameters indicate an environment favourable for cold-pool development and triggering of convective cells upstream of the mountains. As observed during the M2007 and M2009 events, stationary deep convection develops and persists on the same area as the convective cold-pool propagation is nearly balanced by the environmental inflow. Only IOP18 does not fit completely with the theoretical results. Low-CAPE values and strong wind speed make this case quite particular and it is difficult to refer it to idealised simulations proposed in the literature. However, for all the three Upstream events the

evaporative cooling beneath the precipitation system plays only a secondary role in determining the characteristics of the convective system. Indeed, stationarity of the convergence line and of the convection upstream of the Alps is mainly ascribable to the persistence of blocked-flow conditions. For these events, convective outflow can only slightly modify rainfall position and intensity.

Finally, h_m/LFC is also computed for the Alpine events during the intense precipitation phase, when the thermodynamic profile of the impinging flow becomes unstable. Here, h_m/LFC confirms the possible development of convection, embedded in the orographic stratiform precipitation, responsible for locally enhancing the rain rates.

Several other aspects will be explored in future studies. The role of neighbouring mountain ranges (Apennines and Dinaric Alps) will be investigated as well as the role of intense air-sea interactions on water vapour budget and boundary layer characteristics. Moreover, the analysis of additional heavy-precipitation events will possibly provide a more robust statistical support to these results.

Acknowledgements: This work represents a contribution to the HyMeX program. This work was supported by the Italian flagship project RITMARE. The authors are grateful to two anonymous reviewers for their pertaining remarks and comments, which helped improve this manuscript. The authors thank Dr. Anna Fornasiero for providing radar images during the early stages of the study, and Dr. Mario Miglietta, Dr. Andrew Barrett and Dr Andrea Buzzi for fruitful discussions and relevant suggestions. Thanks also to Nick Byrne for having carefully read the manuscript. The authors wish to thank all the participants to the Italian national operational centre during the SOP1 field campaign: CNR (ISAC, IBIMET, IMAA), CETEMPS, Università La Sapienza, ISPRA, Università Parthenope, OSMER-ARPA FVG, ARPA Piemonte, ARPAV, ARPA-SIMC, LaMMA, ARPAL, Centro Funzionale Abruzzo, Centro Funzionale Marche, Centro Funzionale Umbria. Thanks also to the National Department of Civil Protection (DPC) and to the CIMA foundation for providing data of the national raingauge and radar network.

REFERENCES

Barbi A, Monai M, Racca R, Rossa AM. 2012. Recurring features of extreme autumnal rainfall events on the Veneto coastal area. *Nat. Hazards Earth Syst. Sci.* **12**: 2463-2477.

Barrett A, Gray S, Kirshbaum D, Nigel R, Schultz D, Fairman JG. 2014. Synoptic versus orographic control on stationary convective banding. *Q. J. R. Meteorol. Soc.* **141**: 1101-1113.

Billet S, Toro EF. 1997. On WAF-type schemes for multidimensional hyperbolic conservation laws. *J. Comput. Phys.* **130**: 1–24.

Borga M, Boscolo P, Zanon F, Sangati M. 2007. Hydrometeorological analysis of the 29 August 2003 flash flood in the Eastern Italian Alps. *J. Hydrometeorol.* **8**: 1049-1067.

Bougeault P, Binder P, Buzzi A, Dirks R, Kuettner J, Smith RB, Steinacker R, Volkert H. 2001. The MAP special observing period. *Bull. Amer. Meteorol. Soc.* **82**: 433-462.

Bousquet O, Smull BF. 2003. Observations and impacts of upstream blocking during a widespread orographic precipitation event. *Q. J. R. Meteorol. Soc.* **129:** 391-410.

Bresson R, Ricard D, Ducrocq V. 2009. Idealized mesoscale numerical study of Mediterranean heavy precipitating convective systems. *Meteorol. Atmos. Phys.* **103**: 45-55.

Bresson R, Ducrocq V, Nuissier O, Ricard D, de Saint-Aubin C. 2012. Idealized numerical simulations of quasi-stationary convective systems over the Northwestern Mediterranean complex terrain. *Q. J. R. Meteorol. Soc.* **138**: 1751-1763.

Buzzi A. 2004. Heavy precipitation and Alpine orography. In *Proceedings of the International Workshop on timely warnings of heavy precipitation episodes and flash floods*, Ljubljana, Slovenia, 12pp.

Buzzi A, Foschini L. 2000. Mesoscale meteorological features associated with heavy precipitation in the southern Alpine region. *Meteorol. Atmos. Phys.* **72**: 131-146.

Buzzi A, D'Isidoro M, Davolio S. 2003. A case study of an orographic cyclone south of the Alps during the MAP SOP. *Q. J. R. Meteorol. Soc.* **129**: 1795-1818.

Buzzi A, Davolio S, Malguzzi P, Drofa O, Mastrangelo D. 2014. Heavy rainfall episodes over Liguria of autumn 2011: numerical forecasting experiments. *Nat. Hazards Earth Syst. Sc.* **14**: 1325-1340.

Chen SH, Lin YL. 2005. Effects of moist Froude number and CAPE on a conditionally unstable flow over a mesoscale mountain ridge. *J. Atmos. Sci.* **62**: 331-350.

Davolio S, Buzzi A, Malguzzi P. 2009a. Orographic triggering of long-lived convection in three dimensions. *Meorol. Atmos. Phys.*, **103**, 35-44.

Davolio S, Mastrangelo D, Miglietta MM, Drofa O, Buzzi A, Malguzzi P. 2009b. High resolution simulations of a flash flood near Venice. *Nat. Hazards Earth Syst. Sci.* **9**: 1671-1678.

Davolio S, Miglietta MM, Diomede T, Marsigli C, Montani A. 2013. A flood episode in Northern Italy: multi-model and single-model mesoscale meteorological ensembles for hydrological predictions. *Hydrol. Earth Syst. Sci.* **17**: 1-14.

Davolio S, Ferretti R, Baldini L, Casaioli M, Cimini D, Ferrario ME, Gentile S, Loglisci N, Maiello I, Manzato A, Mariani S, Marsigli C, Marzano FS, Miglietta MM, Montani A, Panegrossi G, Pasi F, Pichelli E, Pucillo A, Zinzi A. 2015. The role of the Italian scientific community in the first HyMeX SOP: an outstanding multidisciplinary experience. *Meteorol. Zeit.*, doi:10.1127/metz/2015/0624.

Di Muzio E. 2014: Climatological characterization and dynamics of barrier winds in the Italian region. *PhD Thesis*, http://amslaurea.unibo.it/6688 (accessed 02 October 2015).

Doswell CA, Ramis C, Romero R, Alonso S. 1998. A diagnostic study of three heavy precipitation episodes in the western Mediterranean. *Weather Forecasting*. **13**: 102-124.

Drobinski P, Ducrocq V, Alpert P, Anagnostou E, Béranger K, Borga M, Braud I, Chanzy A, Davolio S, Delrieu G, Estournel C, Filali Boubrahmi N, Font J, Grubisic V, Gualdi S, Homar V, Ivancan-Picek B, Kottmeier C, Kotroni V, Lagouvardos K, Lionello P, Llasat MC, Ludwig W, Lutoff C, Mariotti A, Richard E, Romero R, Rotunno R, Roussot O, Ruin I, Somot S, Taupier-Letage I, Tintore J, Uijlenhoet R, Wernli H. 2014. HyMeX, a 10-year multidisciplinary program on the Mediterranean water cycle. *Bull. Amer. Meteorol. Soc.* **95**: 1063-1082.

Drofa OV, Malguzzi P. 2004. Parameterization of microphysical processes in a non hydrostatic prediction model. In *Proceedings of 14th International Conference on Clouds and Precipitation*, Bologna, Italy, 1297-1300.

Ducrocq V, Braud I, Davolio S, Ferretti R, Flamant C, Jansa A, Kalthoff N, Richard E, Taupier-Letage I, Ayral PA, Belamari S, Berne A, Borga M, Boudevillain B, Bock O, Boichard JL, Bouin MN, Bousquet O, Bouvier C, Chiggiato J, Cimini D, Corsmeier U, Coppola L, Cocquerez P, Defer E, Delanoë J, Di Girolamo P, Doerenbecher A, Drobinski P, Dufournet Y, Fourrié N, Gourley JJ, Labatut L, Lambert D, Le Coz J, Marzano FS, Molinié G, Montani A, Nord G, Nuret M, Ramage K, Rison B, Roussot O, Said F, Schwarzenboeck A, Testor P, Van Baelen J, Vincendon B, Aran M, Tamayo J. 2014. HyMeX-SOP1, the field campaign dedicated to heavy precipitation and flash flooding in the northwestern Mediterranean. *Bull. Amer. Meteorol. Soc.* **95**: 1083-1100.

Emanuel K. A. 1994. Atmospheric Convection. Oxford University Press, 580 pp.

Ferretti R, Pichelli E, Gentile S, Maiello I, Cimini D, Davolio S, Miglietta MM, Panegrossi G, Baldini L, Pasi F, Marzano FS, Zinzi A, Mariani S, Casaioli M, Bartolini G, Loglisci N, Montani A, Marsigli C, Manzato A, Pucillo A, Ferrario ME, Colaiuda V, Rotunno R. 2014. Overview of the first HyMeX Special Observation Period over Italy: observations and model results. *Hydrol. Earth Syst. Sci.* **18**:1953-1977.

Frei C, Schär C. 1998. A precipitation climatology of the Alps from high-resolution rain-gauge observations. *Int. J. Climatol.* **18**: 873-900.

Galway JG. 1956. The lifted index as a predictor of latent instability. *Bull. Amer. Meteorol. Soc*. **37**: 528-529.

Isotta FA, Frei C, Weilguni V, Percec Tadic M, Lassegues P, Rudolf B, Pavan V, Cacciamani C, Antolini G, Ratto SM, Munari M, Micheletti S, Bonati V, Lussana C, Ronchi C, Panettieri E, Marigo G, Vertacnik G. 2013. The climate of daily precipitation in the Alps: development and analysis of a high-resolution grid dataset from pan-Alpine rain-gauge data. *Int. J. Climatol.* **34**: 1657-1675.

Kain JS. 2004. The Kain-Fritsch convective parameterization: an update. *J. Appl. Meteorol.* **43**: 170-181.

Lin YL, Reeves HD, Chien SY, Chiao S. 2005. Formation mechanisms for convection over Ligurian Sea during MAP IOP-8. *Mon. Weather Rev.* **133**: 2227-2245.

Malguzzi P, Grossi G, Buzzi A, Ranzi R, Buizza R. 2006. The 1966 'century' flood in Italy: A meteorological and hydrological revisitation. *J. Geophys. Res.* **111**: D24106, doi:10.1029/2006JD007111.

Manzato A. 2003. A climatology of instability indices derived from Friuli Venezia Giulia soundings, using three different methods. *Atmos. Res.* **67-68**: 417-454.

Manzato A. 2007. The 6 h climatology of thunderstorms and rainfalls in the Friuli Venezia Giulia plain. *Atmos. Res.* **83**: 336-348.

Manzato A, Davolio S, Miglietta MM, Pucillo A, Setvak M. 2015. 12 September 2012: A supercell outbreak in NE Italy? *Atmos. Res.* **153**: 98-118.

Manzato A, Cicogna A, Pucillo A. 2015. 6-hour maximum rain in Friuli Venezia Giulia: climatology and ECMWF-based forecasts. *Atmos. Res.* doi:10.1016/j.atmosres.2015.07.013 In press.

Massacand AC, Wernli H, Davies HC. 1998. Heavy precipitation on the Alpine southside: an upper-level precursor. *Geophys. Res. Lett.* **25:** 1435-1438.

Mazòn J, Pino D. 2013. The role of sea-land air thermal difference, shape of the coastline and sea surface temperature in the nocturnal offshore convection. *Tellus A* **65**: 1-13.

Miglietta MM, Buzzi A. 2004. A numerical study of moist stratified flow regimes over isolated topography. *Q. J. R. Meteorol. Soc.* **130**: 1749-1770.

Miglietta MM, Rotunno R. 2005. Simulations of moist nearly neutral flow over a ridge. *J. Atmos. Sci.* **62**: 1410-1427.

Miglietta MM, Rotunno R. 2009. Numerical simulations of conditionally unstable flows over a ridge. *J. Atmos. Sci.* **66**: 1865-1885.

Miglietta MM, Rotunno R. 2010. Numerical simulations of low-CAPE flows over a mountain ridge. *J. Atmos. Sci.* **67**: 2391-2401.

Miglietta MM, Rotunno R. 2014. Numerical simulations of sheared conditionally unstable flows over a mountain ridge. *J. Atmos. Sci.* **71**: 1747-1762.

Morcrette JJ, Barker HW, Cole JNS, Iacono MJ, Pincus R. 2008. Impact of a new radiation package, McRad, in the ECMWF Integrated Forecasting System. *Mon. Weather. Rev.* **136**: 4773-4798.

Monai M, Rossa AM, Bonan C. 2006. Partitioning of snowy and rainy precipitation in a case of a north Adriatic frontal passage. *Advances in Geosciences* **7**: 279-284.

Nuissier O, Ducrocq V, Ricard D, Lebeaupin C, Anquetin S. 2008. A numerical study of three catastrophic precipitating events over southern France. I: Numerical framework and synoptic ingredients. *Q. J. R. Meteorol. Soc.* **134**: 111-130.

Pierrehumbert RT, Wyman B. 1985. Upstream effects of mesoscale mountains. *J. Atmos. Sci.* **42**: 977-1003.

Ricard D, Ducrocq V, Auger L. 2012. A climatology of the mesoscale environment associated with heavily precipitating events over a northwestern Mediterranean area. *J. Appl. Meteorol. Climatol.* **51**: 468-488.

Rudari R, Entekhabi D, Roth G. 2004. Terrain and multiple-scale interactions as factors in generating extreme precipitation events. *J. Hydrometeorol.* **5**, 390–404.

Ritter B, Geleyn JF. 1992. A comprehensive radiation scheme for numerical weather prediction models with potential applications in climate simulations. *Mon. Weather. Rev.* **120**: 303-325.

Rossa AM, Cenzon G, Monai M. 2010. Quantitative comparison of radar QPE to rain gauges for the 26 September 2007 Venice Mestre flood. *Nat. Hazards Earth Syst. Sci.* **10**: 371-377.

Rotach MW, Ambrosetti P, Ament F, Appenzeller C, Arpagaus M, Bauer HS, Behrendt A, Bouttier F, Buzzi A, Corazza M, Davolio S, Denhard M, Dorninger M, Fontannaz L, Frick J, Fundel F, Germann U, Gorgas T, Hegg C, Hering A, Keil C, Liniger MA, Marsigli C, McTaggart-Cowan R,

Montani A, Mylne K, Ranzi R, Richard E, Rossa A, Santos-Muñoz D, Schär C, Seity Y, Staudinger M, Stoll M, Volkert H, Walser A, Wang Y, Werhahn J, Wulfmeyer V, Zappa M. 2009. MAP D-PHASE: Real-time Demonstration of Weather Forecast Quality in the Alpine Region. *Bull. Amer. Meteorol. Soc.* **90**: 1321-1336.

Rotunno R, Ferretti R. 2001. Mechanisms of intense Alpine rainfall. *J. Atmos. Sci.* **58**: 1732-1749.

Rotunno R, Ferretti R. 2003. Orographic effects on rainfall in MAP cases IOP2b and IOP8. *Q. J. R. Meteorol. Soc.* **129**: 373-390.

Rotunno R, Houze RA. 2007. Lessons on orographic precipitation from the Mesoscale Alpine Programme. *Q. J. R. Meteorol. Soc.* **133**: 811-830.

Schwerdtfeger W. 1984. Weather and Climate of the Antarctic. Elsevier Sciences Publisher, 261 pp.

Smith RB. 1979. The influence of mountains on the atmosphere. *Advances in Geophysics* **21**: 87-230.

Setvák M, Bedka K, Lindsey DT, Sokol A, Charvát Z, Šťástka J, Wang PK. 2013. A-Train observations of deep convective storm tops. *Atmos. Res.* **123**: 229-248.

Smolarkiewicz PK, Rotunno R. 1990. Low Froude number flow past three-dimensional obstacles. Part II: Upwind flow reversal zone. *J. Atmos. Sci.* **47:** 1498-1511.

Zampieri M, Malguzzi P, Buzzi A. 2005. Sensitivity of quantitative precipitation forecasts to boundary layer parameterization: a flash flood case study in the Western Mediterranean. *Nat. Hazards Earth Syst. Sci.* **5**: 603-612.

Event name (Acronym) Type of event	Initial Condition for BOLAM	Initial Condition for MOLOCH	Max Rainfall Observation (Simulation) Accumulation period
HyMeX - IOP19 (IOP19) Alpine	04 November 2012 00 UTC	04 November 2012 03 UTC	370 (350) mm/30h 04 Nov, 06 UTC – 05 Nov. 12 UTC
Piancavallo 2012 (P2012) Alpine	10 November 2012 12 UTC	10 November 2012 15 UTC	390 (310) mm/24h 11 Nov, 00 UTC – 12 Nov, 00 UTC
Vicenza 2010 (V2010) Alpine	30 October 2010 18 UTC	30 October 2010 21 UTC	600 (600) mm/48h 31 Oct, 00 UTC – 02 Nov, 00 UTC
HyMeX - IOP18 (IOP18) Upstream	31 October 2012 00 UTC	31 October 2012 06 UTC	120 (140) mm/24h 31 Oct, 12 UTC – 01 Nov, 12 UTC
Marghera 2007 (M2007) Upstream	25 September 2007 12 UTC	25 September 2007 18 UTC	320 (330) mm/12h 26 Sep. 00 UTC – 26 Sep. 12 UTC
Mira 2009 (M2009) Upstream	15 September 2009 18 UTC	16 September 2009 00 UTC	180 (210) mm/24h 16 Sep 00 UTC – 17 Sep 00 UTC

Table 1: List of analysed events and their acronyms, initialization time for BOLAM and MOLOCH simulations, accumulated (observed and forecast) precipitation and selected rainfall accumulation period.

Alpine event	Analysed time	Initiation of intense precipitation	CAPE ($J\ kg^{-1}$)	Lifted Index (K)	h_b (m)	U ($m\ s^{-1}$)
IOP19	04 Nov 2012 15 UTC	04 Nov 2012 18 UTC	100	2.2	480	13.2
P2012	10 Nov 2012 18 UTC	11 Nov 2012 00 UTC	3	4.6	500	12.3
V2010	31 Oct 2010 03 UTC	31 Oct 2010 06 UTC	40	4.3	480	12.1

Table 2: Summary of parameters computed for the triggering phase for the three Alpine events. Convective Available Potential Energy (CAPE), Lifted Index (LI), depth of the stable layer characterised by barrier wind over the NEI plain (h_b), meridional component of the wind averaged among the model levels below 2000 m (U). The most unstable parcel was used in the computation.

Upstream event	Analysed time	Initiation of intense precipitation	CAPE (J kg^{-1})	Lifted Index (K)	LFC (m)	h_b (m)	h_b/LFC	h_m/LFC	U (m s^{-1})	DCAPE (J kg^{-1})	CAPE$^{1/2}$/U	DCAPE$^{1/2}$/U	N LFC/U
IOP18	31 Oct 2012 20 UTC	31 Oct 2012 22 UTC	190	0.5	340	780	2.3	5.9	22.8	120	0.6	0.5	0.15
M2007	26 Sep 2007 03 UTC	26 Sep 2007 05 UTC	1190	-3.9	480	480	1.0	4.2	7.4	680	4.7	3.5	0.52
M2009	16 Sep 2007 07 UTC	16 Sep 2009 10 UTC	2060	-5.3	480	600	1.3	4.2	12.4	450	3.7	1.7	0.33

Table 3: Summary of parameters computed for the triggering phase for the three Upstream events. Convective Available Potential Energy (CAPE), Lifted Index (LI), depth of the stable layer characterised by barrier wind over the NEI plain (h_b), ratio between h_b and LFC, ratio between ridge height (h_m = 2000 m) and LFC, meridional component of the wind averaged among the model levels below 2000 m (U), Downdraft Convective Available Potential Energy (DCAPE), CAPE$^{1/2}$/U, DCAPE$^{1/2}$/U, N LFC / U. The most unstable parcel was used in the computation.

FIGURE CAPTIONS

Figure 1: area of interest corresponding to the MOLOCH integration domain and indication of the locations mentioned in the text: Venice (cross), Vicenza (plus), Padua (star), Concordia Sagittaria (dot) SODAR and Campoformido (Udine) sounding (triangle). The NEI area including the Friuli Venezia Giulia (FVG) and Veneto regions is also indicated. Model orography above 1500 meters is shaded.

Figure 2: synoptic situation for the six events (IFS - ECMWF analyses). Geopotential height at 500 hPa (dam, black lines), sea level pressure (hPa, white lines) and temperature at 500 hPa (°C, colour shading). (a) IOP19, 05 Nov. 2012 at 0600 UTC; (b) Piancavallo event, 11 Nov. 2012 at 0600 UTC; (c) Vicenza event, 01 Nov. 2010 at 0000 UTC; (d) IOP18, 31 Oct. 2012 at 1200 UTC; (e) Marghera event, 26 Sep. 2007 at 0600 UTC; (f) Mira event, 16 Sep. 2009 at 1200 UTC.

Figure 3: observed precipitation, obtained by interpolation of data provided by the dense networks of Veneto (about 170 rain-gauges) and FVG (about 260 rain-gauges) regional meteorological agencies, for the six events. (a) IOP19, 30-h accumulated precipitation at 1200 UTC, 05 Nov. 2012; (b) Piancavallo event, 24-h accumulated precipitation at 0000 UTC, 12 Nov. 2012; (c) Vicenza event, 48-h accumulated precipitation at 0000 UTC, 02 Nov. 2010; (d) IOP18, 24-h accumulated precipitation at 1200 UTC, 01 Nov. 2012; (e) Marghera event, 12-h accumulated precipitation at 1200 UTC, 26 Sep. 2007; (f) Mira event, 24-h accumulated precipitation at 0000 UTC, 17 Sep. 2009. The regional border of Veneto and FVG regions are also plotted.

Figure 4: as in Fig. 3, but for MOLOCH forecasts.

Figure 5: (a) High-resolution SODAR wind data in Concordia Sagittaria between 0300 and 1200 UTC, 31 Oct. 2010 (V2010 event). (b) High-resolution SODAR wind data in Padua between 0000 and 1200 UTC, 26 Sep. 2007 (M2007 event). Note that the time reported on the x-axis are in CET, corresponding to UTC+1.

Figure 6: evolution of the Froude number for the six heavy-precipitation events over the Alps, Hours on x-axis are referred to the initiation of intense precipitation. Dashed (solid) lines for the Upstream (Alpine) events.

Figure 7: MOLOCH 10-meter wind (m s^{-1}, shading) during the initial stage of the events, when the Sirocco wind is blocked by the orography and deflected as barrier wind ahead of the Alps: (a) Vicenza event, 31 Oct. 2010, 0300 UTC; (b) Marghera event, 26 Sep. 2007, 0400 UTC. The black dashed lines indicate the location of the vertical cross-sections shown in Fig. 8. The black square indicates the area where averaged vertical profiles are computed. During the precipitation stage of the events: (c) flow-over condition for the Vicenza event, 31 Oct. 2010, 1800 UTC; (d) persisting blocked-flow condition for the Marghera event, 26 Sep. 2007, 1200 UTC. Note that only a portion of the MOLOCH integration domain is shown. Black contours show the 500 m and 1500 m orography elevation.

Figure 8: MOLOCH vertical cross-sections along the black line indicated in Fig. 7. Equivalent potential temperature (thin contour line and colour shading, interval 2 K), tangent wind component (vectors) and cloud water and ice (thick contour indicating 0.1 g kg^{-1}), for Vicenza event (cross section length 314 km), (a) 31 Oct. 2010, 0300 UTC and (c) 01 Nov. 2010, 1000 UTC; Marghera event (cross section length 363 km), 26 Sep. 2007, (b) at 0400 UTC and (d) at1200 UTC.

Figure 9: vertical thermodynamic profiles simulated by MOLOCH during the initial stage of the events and computed as an average over an area of about 15 x 15 km for (a) Vicenza event, 31 Oct. 2010, 0300 UTC, in 45.1 °N, 12.9 °E; (b) Marghera event, 26 Sep. 2007, 0400 UTC, in 45 °N, 13 °E.

Figure 10: profiles of buoyancy for air parcels raised to a height of 500 m above their initial position (vertical axis). Profiles are computed for the initial stage of the events, before intense precipitation occurrence. Dashed (solid) lines for the Upstream (Alpine) events. Values on the x-axis are multiplied by 10^2.

Figure 11: evolution of h_m/LFC for the three Alpine events. Hours on x-axis are referred to the initiation of intense precipitation.

Figure 12: results of MOLOCH simulations performed removing the contribution of evaporation/sublimation of the precipitation (see text). Marghera event (cross section length 363 km): (a) 12-h accumulated precipitation at 1200 UTC, 26 Sep. 2007; (b) vertical cross-sections along the black line of Fig. 7 showing equivalent potential temperature (thin contour line and colour shading, interval 2 K), tangent wind component (vectors) and cloud water and ice (thick contour indicating 0.1 g kg^{-1}) on 26 Sep. 2007 at 1200 UTC.

Figure 13: schematic diagram of the key mechanisms responsible for the two different precipitation patterns over NEI. (a) Upstream event: blocked low-level flow, barrier wind, convergence and deep convection development occurring over the plain, upstream of the orography. (b) Alpine event: unblocked low-level flow, flow-over conditions, orographic lifting and precipitation over the Alps with possible embedded convection.

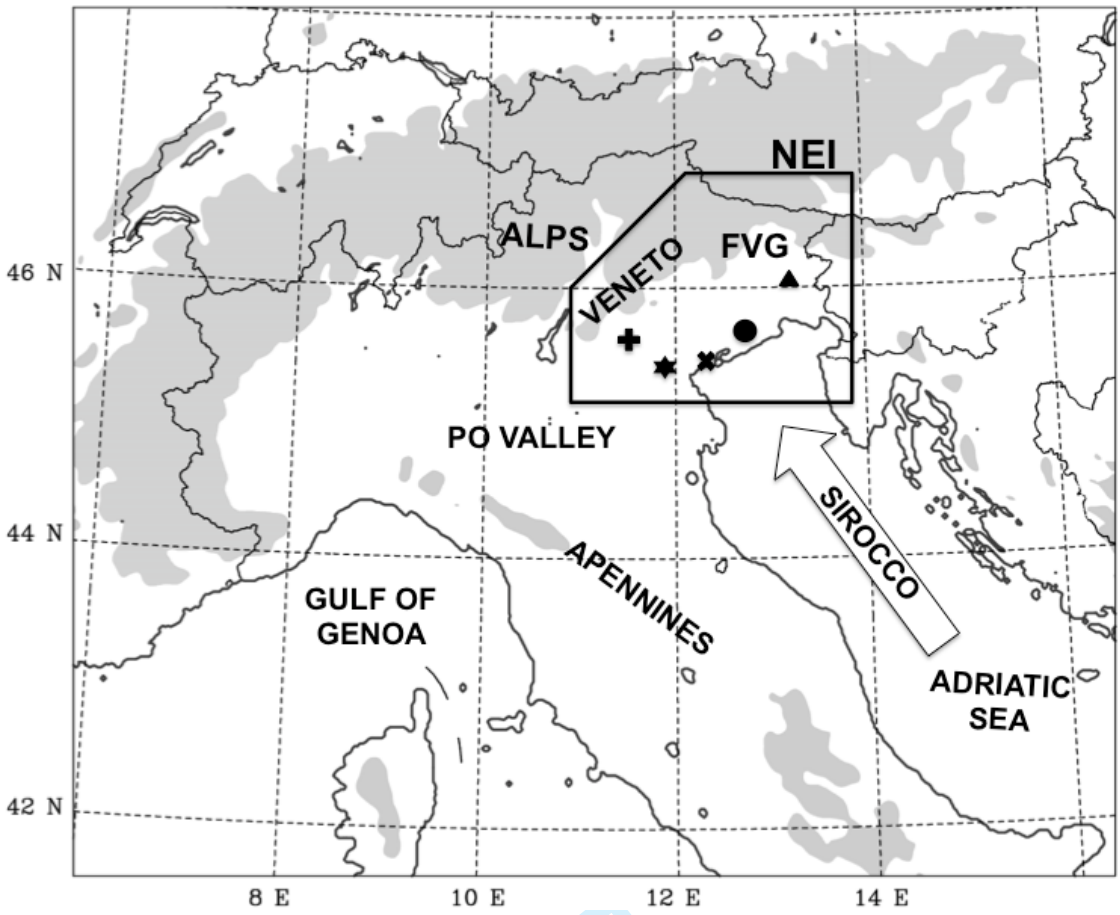

969

970

971 Figure 1

972

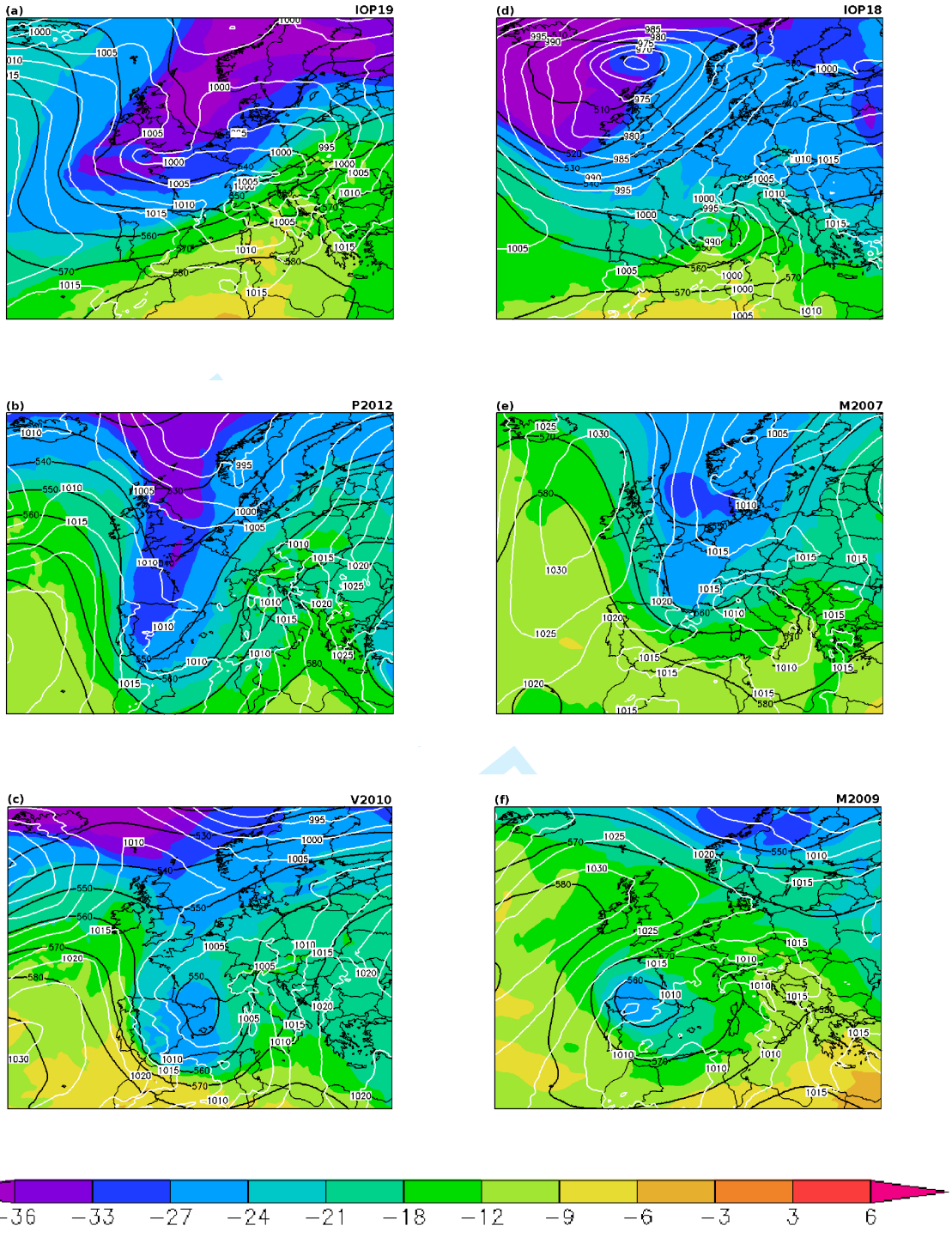
(a) IOP19
(d) IOP18
(b) P2012
(e) M2007
(c) V2010
(f) M2009
−36 −33 −27 −24 −21 −18 −12 −9 −6 −3 3 6

Figure 2

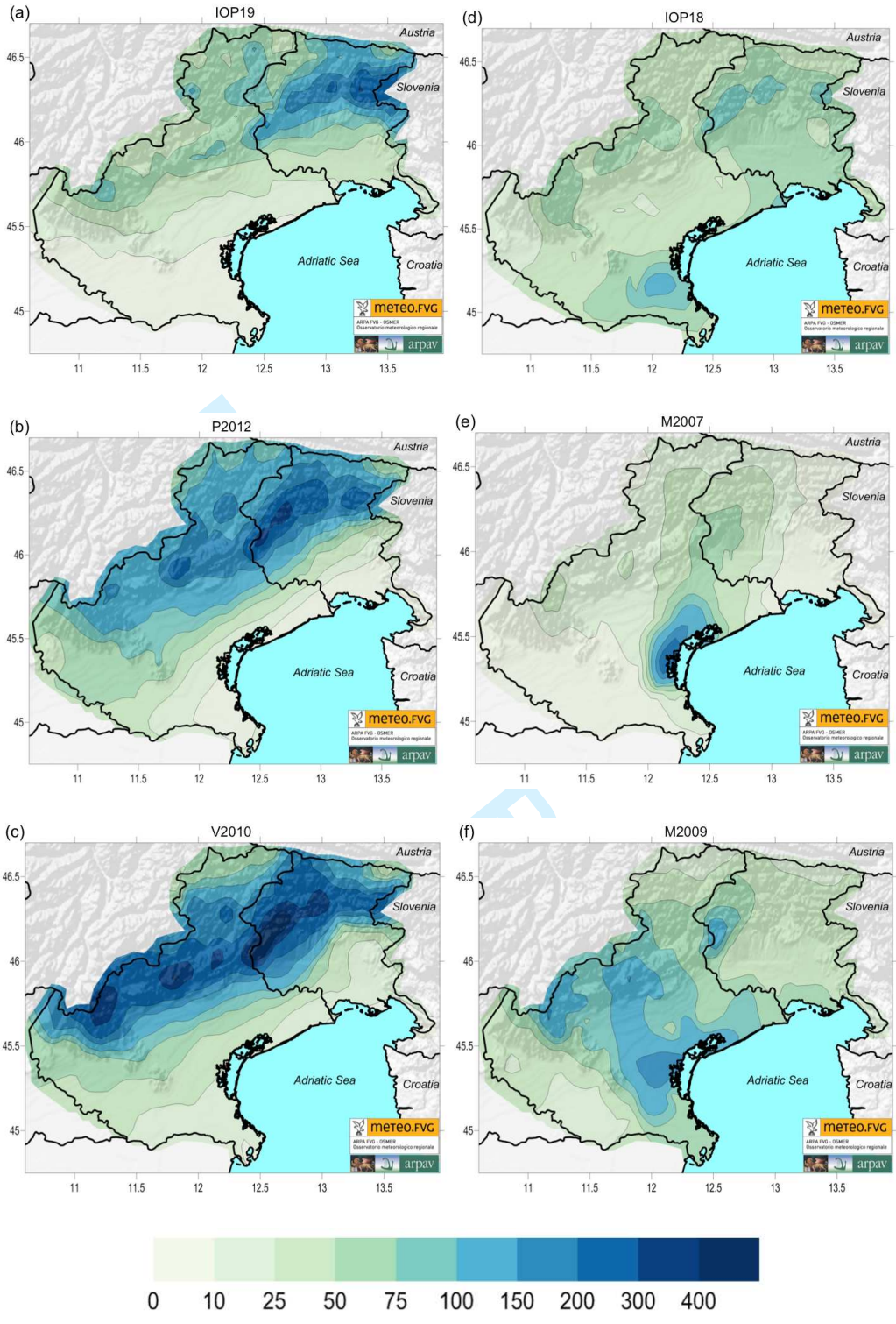
(a)
IOP19
(d)
IOP18
(b)
P2012
(e)
M2007
(c)
V2010
(f)
M2009
Austria
Slovenia
Adriatic Sea
Croatia
meteo.FVG
arpav
46.5
46
45.5
45
11
11.5
12
12.5
13
13.5
0
10
25
50
75
100
150
200
300
400

Figure 3

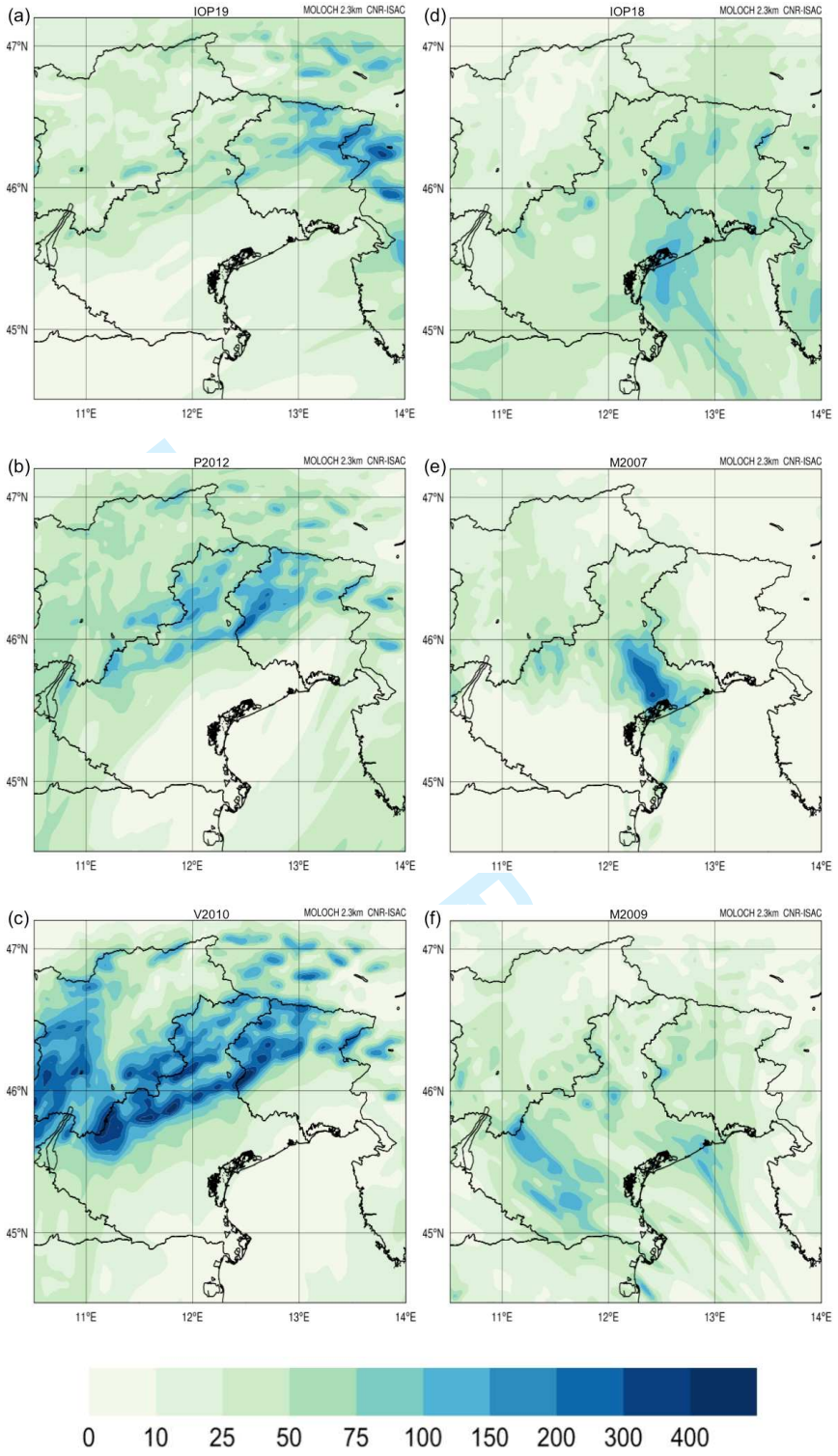
(a) IOP19 MOLOCH 2.3km CNR-ISAC
(d) IOP18 MOLOCH 2.3km CNR-ISAC
(b) P2012 MOLOCH 2.3km CNR-ISAC
(e) M2007 MOLOCH 2.3km CNR-ISAC
(c) V2010 MOLOCH 2.3km CNR-ISAC
(f) M2009 MOLOCH 2.3km CNR-ISAC
47°N
46°N
45°N
11°E
12°E
13°E
14°E
0 10 25 50 75 100 150 200 300 400

Figure 4

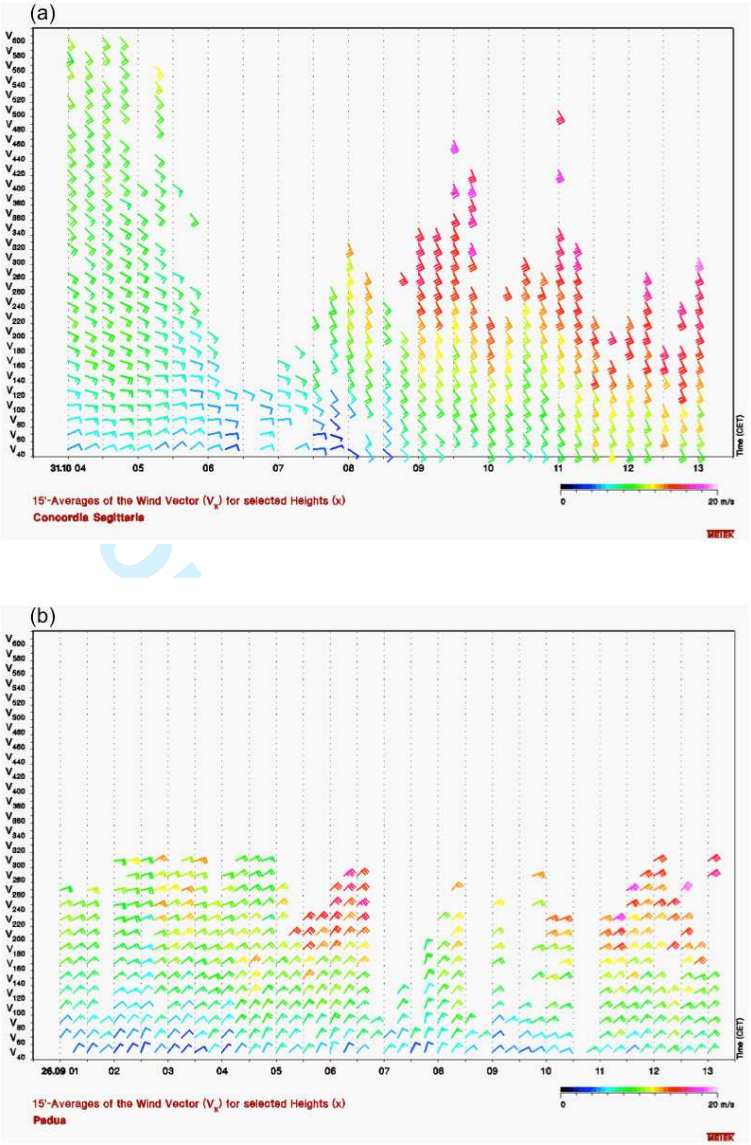

991

992

993 Figure 5

994

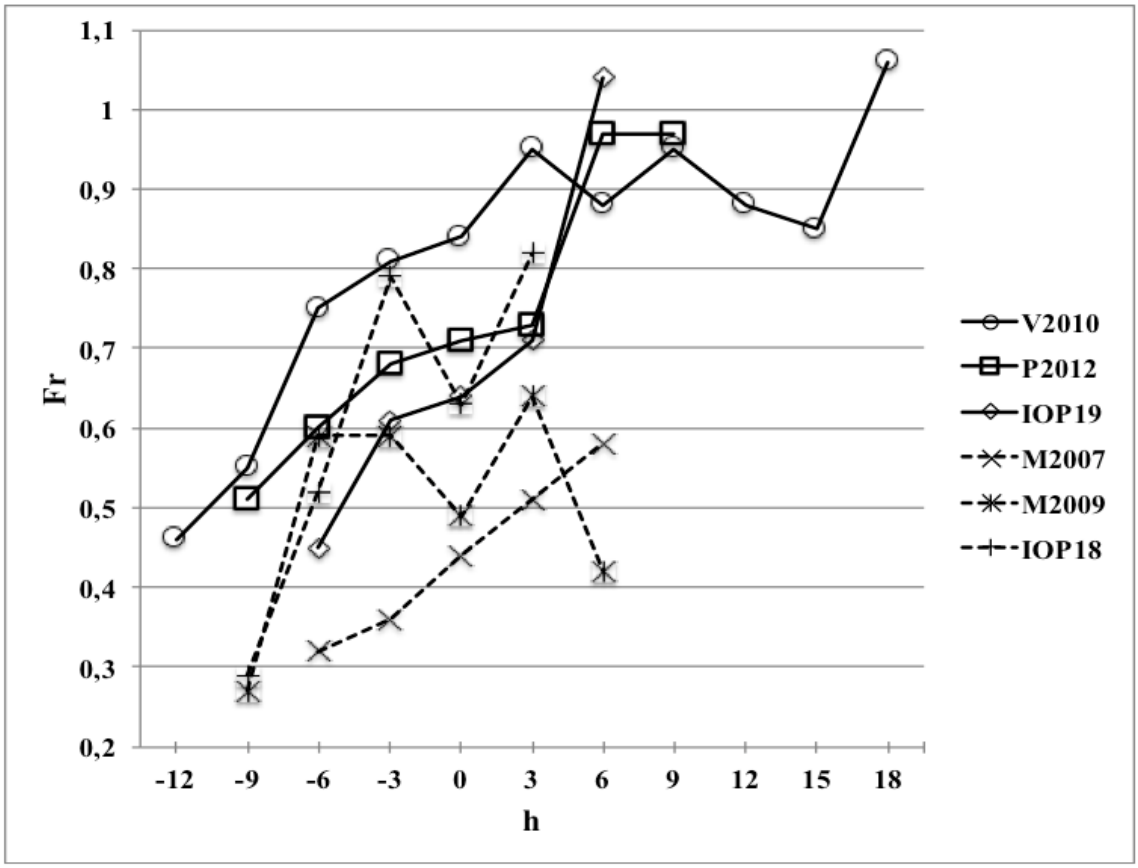

995

996 Figure 6

997

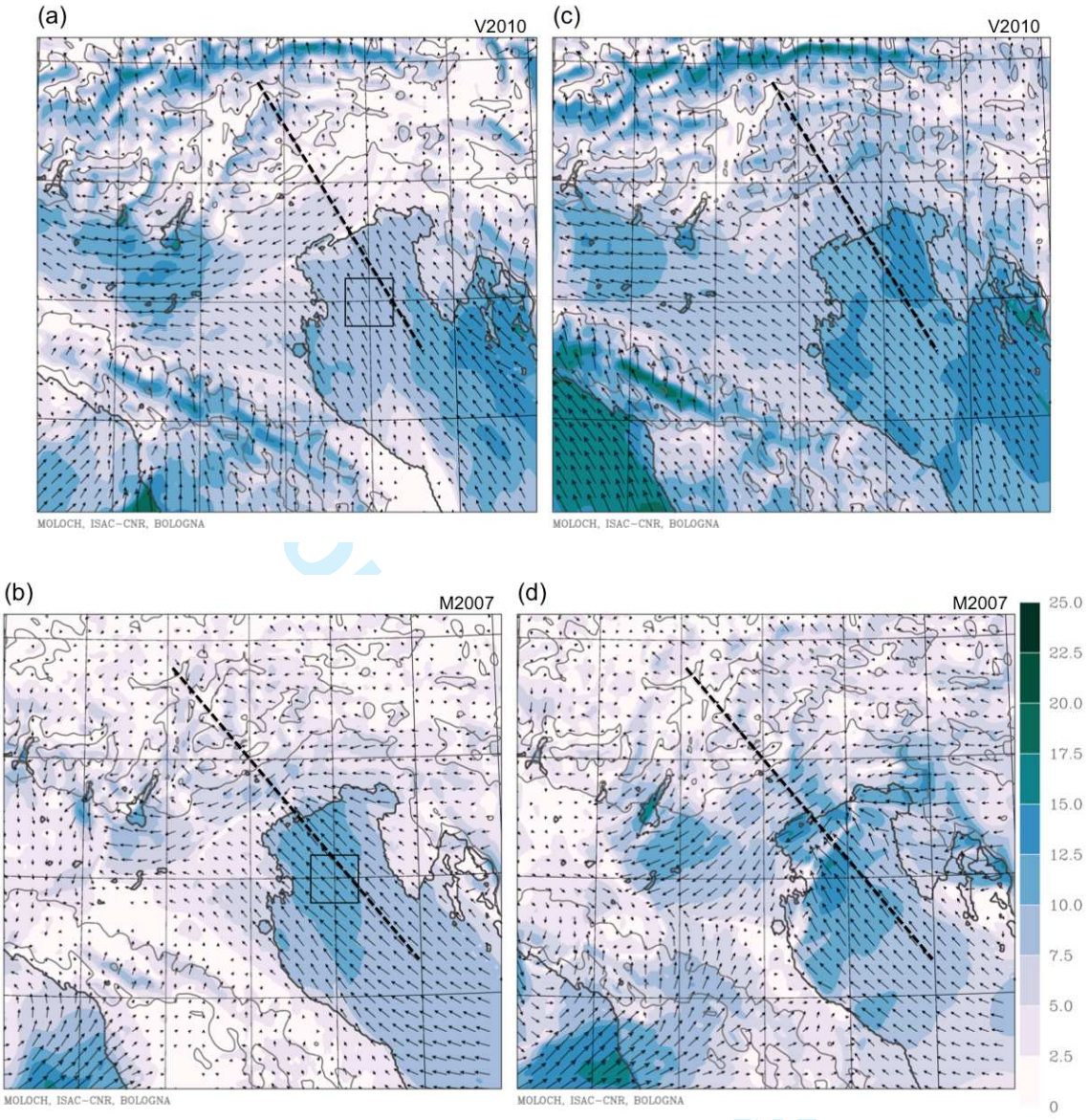
(a)
V2010
(c)
V2010
MOLOCH, ISAC–CNR, BOLOGNA
MOLOCH, ISAC–CNR, BOLOGNA
(b)
M2007
(d)
M2007
25.0
22.5
20.0
17.5
15.0
12.5
10.0
7.5
5.0
2.5
0
MOLOCH, ISAC–CNR, BOLOGNA
MOLOCH, ISAC–CNR, BOLOGNA

Figure 7

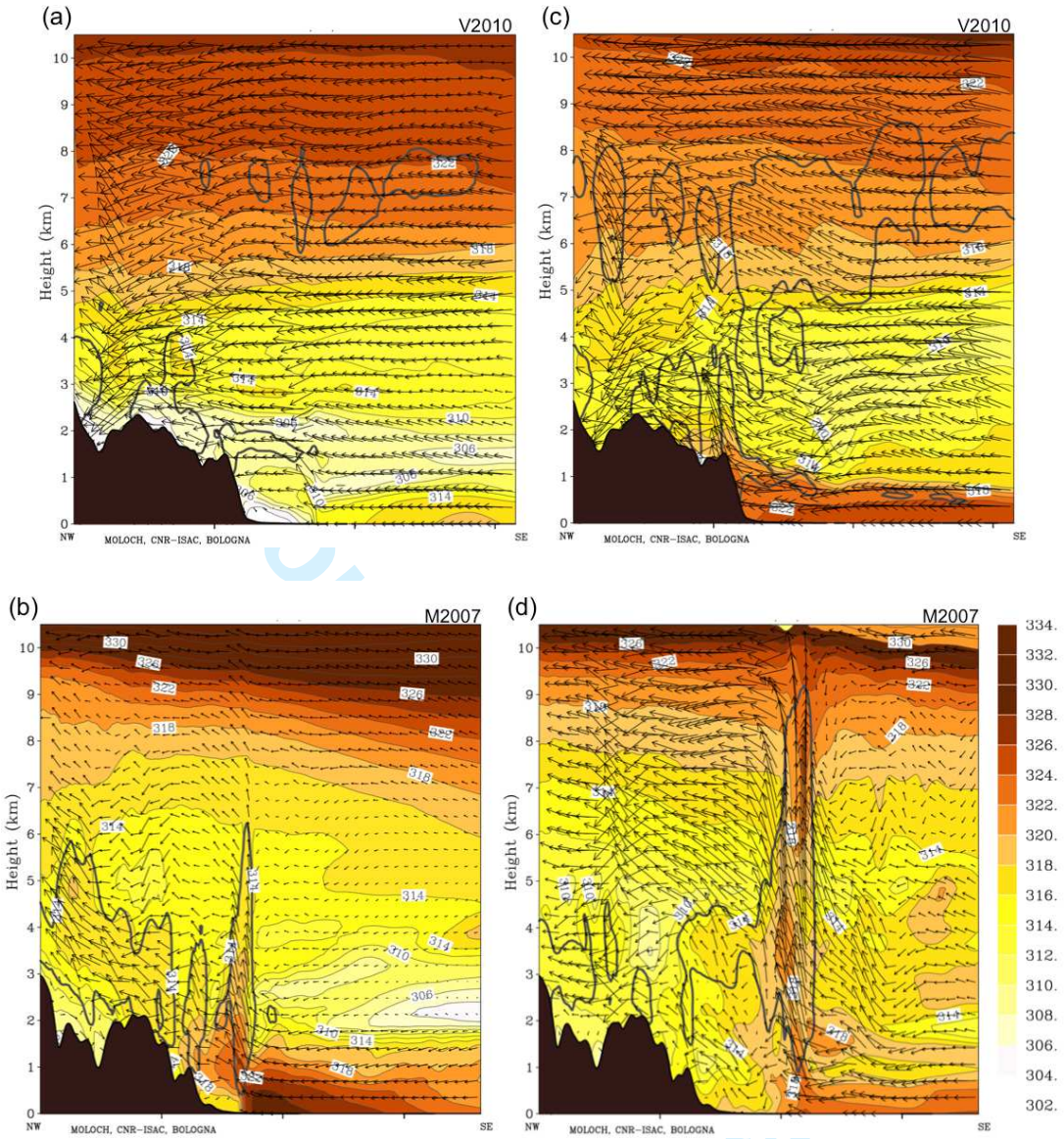
(a)
V2010
(c)
V2010
(b)
M2007
(d)
M2007
Height (km)
NW
SE
MOLOCH, CNR-ISAC, BOLOGNA
334.
332.
330.
328.
326.
324.
322.
320.
318.
316.
314.
312.
310.
308.
306.
304.
302.

Figure 8

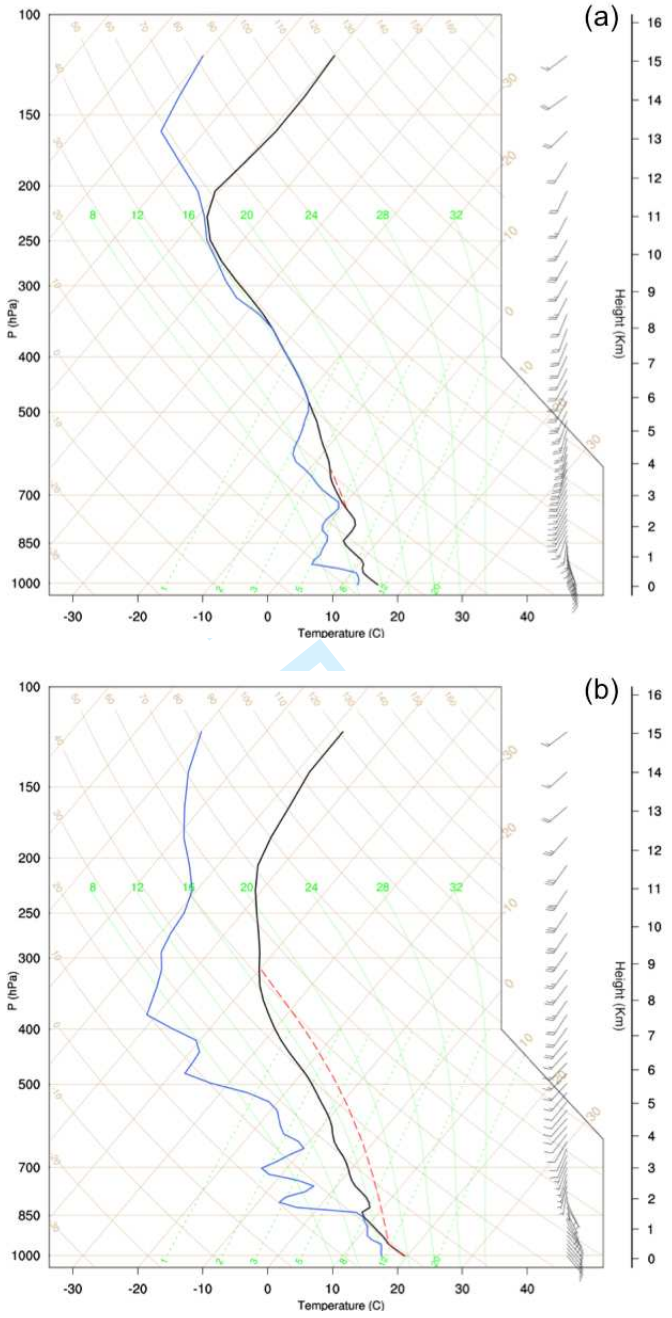
(a)
(b)
P (hPa)
Height (Km)
Temperature (C)
100
150
200
250
300
400
500
700
850
1000
-30
-20
-10
0
10
20
30
40
0
1
2
3
4
5
6
7
8
9
10
11
12
13
14
15
16

Figure 9

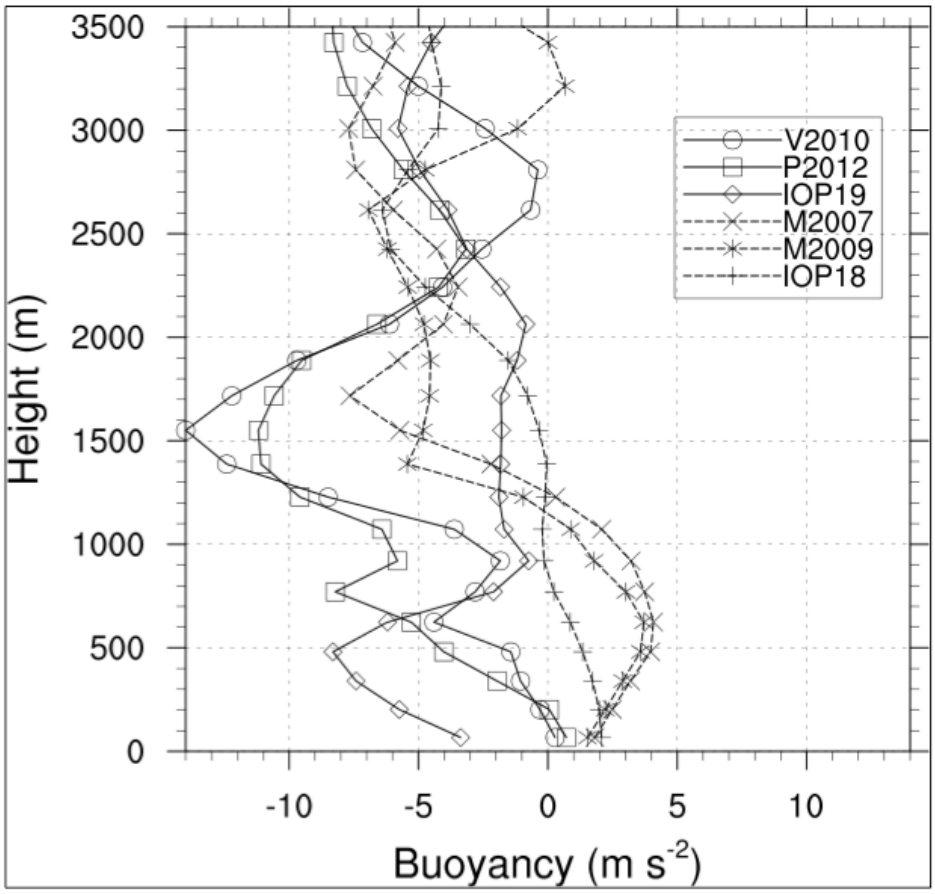

Figure 10

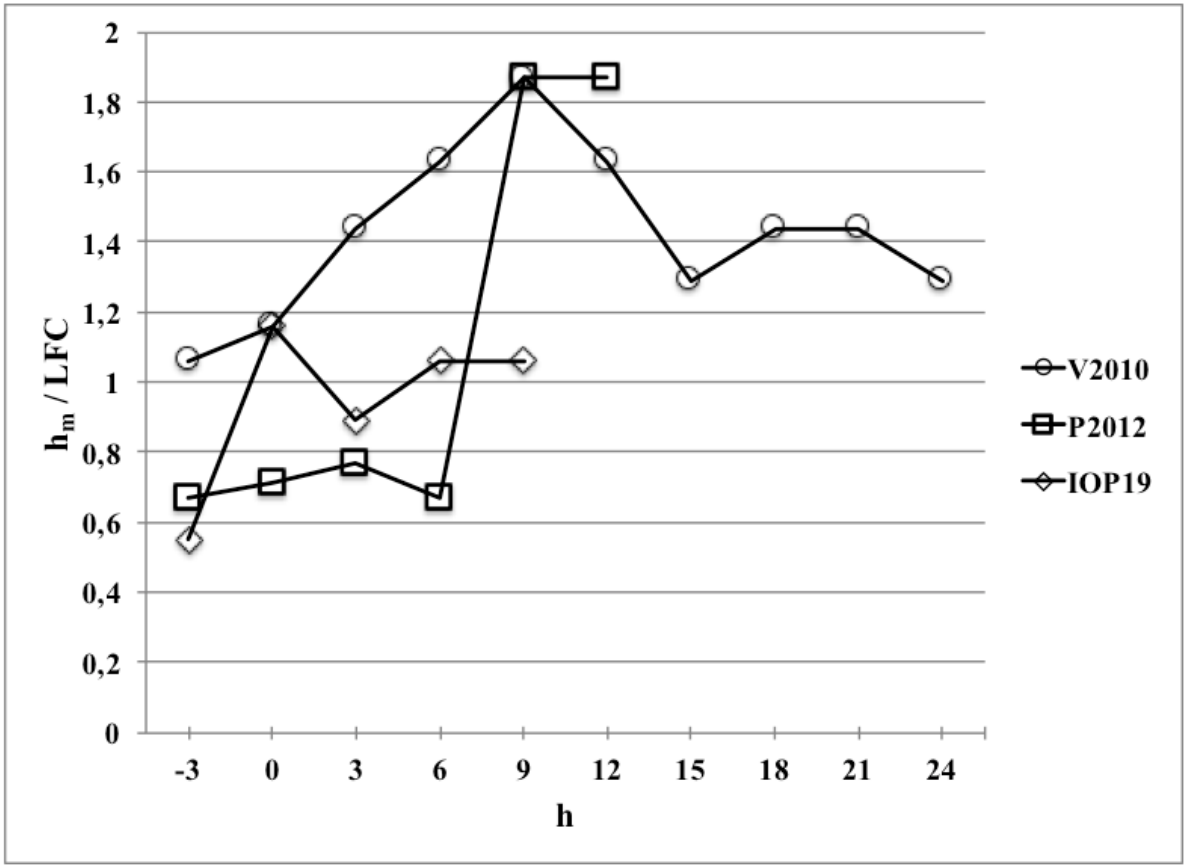

1013

1014 Figure 11

1015

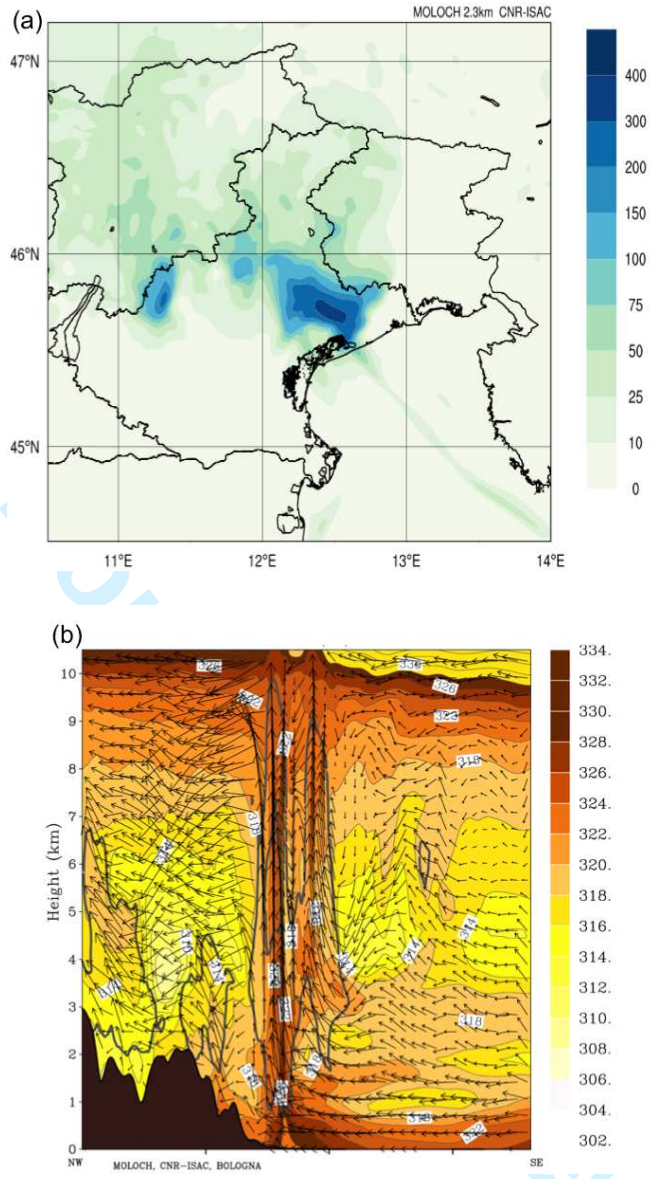
(a)
MOLOCH 2.3km CNR-ISAC
47°N
46°N
45°N
11°E
12°E
13°E
14°E
400
300
200
150
100
75
50
25
10
0
(b)
Height (km)
NW
SE
MOLOCH, CNR-ISAC, BOLOGNA
334.
332.
330.
328.
326.
324.
322.
320.
318.
316.
314.
312.
310.
308.
306.
304.
302.

Figure 12

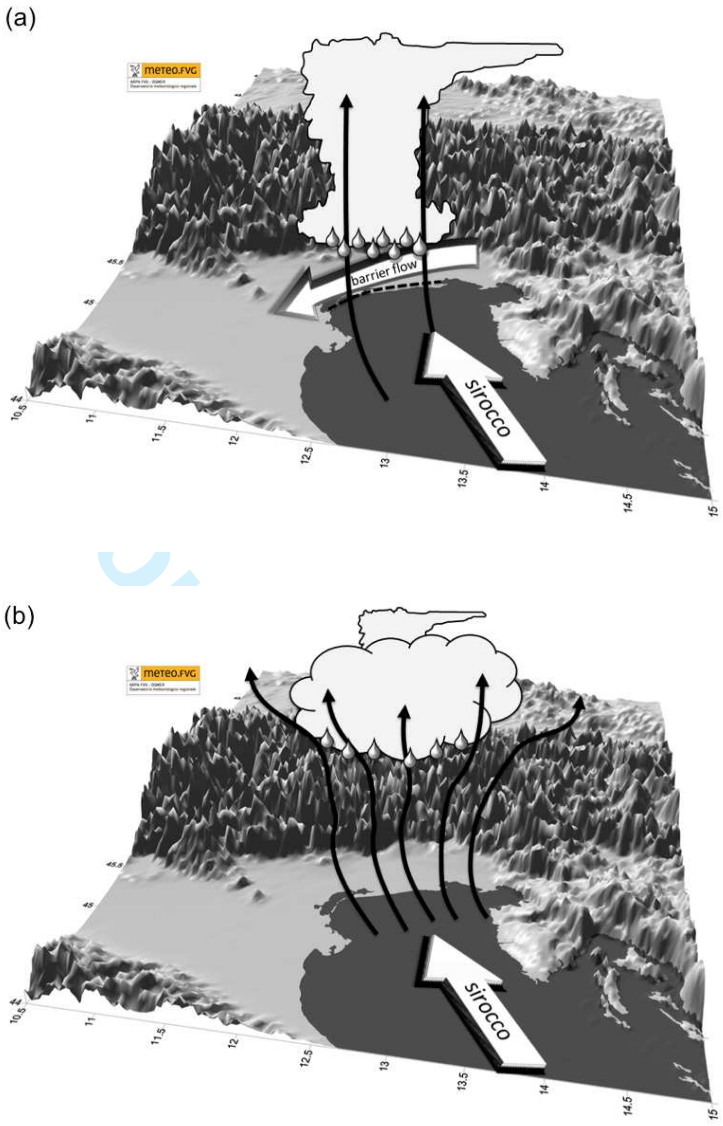

Figure 13